DANISH
TECHNOLOGICAL
INSTITUTE

Mixed refrigerant heat pumps/ cooling systems (MIREHP)

Final report

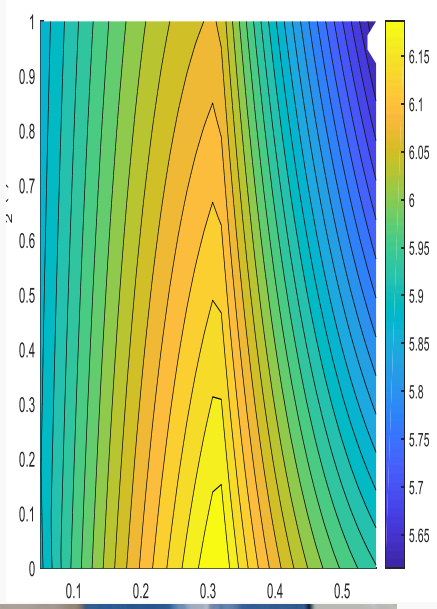

Title:
Mixed refrigerant heat pumps/ cooling systems (MIREHP)

Prepared for:
EUDP, project no. 64016-0045

Prepared by:
Danish Technological Institute
Gregersensvej 2
2630 Taastrup
Refrigeration and Heat Pump Technology

Technical University of Denmark
Niels Koppels Allé, Bygning 403
2800 Kongens Lyngby
Department of Mechanical Engineering

Project consortium:
Sauter
Alfa Laval
danARCTICA
Technical University of Denmark
Danish Technological Institute (project leader)

October 2019

Authors:

Danish Technological Institute:
Claus Madsen
Jóhannes Kristófersson
Christopher Murphy
Benjamin Zühlsdorf
Lars Olsen

Technical University of Denmark:
Brian Elmegaard
Wiebke B. Markussen
Jonas Kjær Jensen

Table of Contents

1. Preface 5
1.1. Project Details 6
1.2. Short Description of Objectives and Results 6
1.3. Executive Summary 7
1.4. Project Objectives 8
1.5. Project Results, Dissemination and Utilization of Results 9
1.6. Utilization of Project Results 9
1.7. Project Conclusion and Perspective 10
2. Introduction 10
3. Final Scientific Dissemination of the Research in the MIREHP Project 12
3.1. Introduction 12
3.2. Subtask 1: Simple Cycle Refrigerant Screening 13
3.2.1. Methods 13
3.2.2. Heat Pump Model 13
3.2.2.1. Thermodynamic Model 13
3.2.2.2. Exergy Analysis 15
3.2.2.3. Refrigerant Screening 17
3.2.3. Results 19
3.2.4. Discussion 26
3.3. Subtask 2: Evaluation of Advanced Cycle Configuration 27
3.3.1. Methods 27
3.3.1.1. Identification of Advanced Cycle Configurations 27
3.3.1.2. Modelling of Advanced Cycle Heat Pump 32
3.3.1.3. Refrigerant Screening 32
3.3.2. Results 33
3.3.2.1. Standard and Suction Gas Heat Exchanger Cycle 33
3.3.2.2. HACHP 34
3.3.2.3. Standard HACHP 34
3.3.2.4. Low Pressure Liquid Circulation 35
3.3.2.5. High Pressure Liquid Circulation 35
3.3.2.6. Refrigerant Screening 36
3.3.2.7. Discussion 40
4. Test of System 43
4.1. Design Considerations 43

4.2. Operation of Tests 45
4.3. Test Results 46
4.3.1. Results with 5 % CO_2 46
4.3.2. Results with 10 % CO_2 49
4.3.3. Results with 15 % CO_2 50
4.4. Evaluation of Test Results 51
5. Conclusion 55
Appendix 1 57
Methodology – obtaining and the utilization of test results 57
Appendix 2. References 60

1. Preface

This report is the final report of the study: "**Mi**xed **re**frigerant **h**eat **p**umps/ cooling systems" (the MIREHP concept). The objective of the project is to develop a new heat pump concept using zeotropic refrigerant mixtures as working medium. By using zeotropic mixtures, a significant boost in system efficiency can be achieved. If an appropriate temperature match is obtained between the refrigerant and brine, and a sufficient heat exchange area is used, a considerable COP enhancement can be obtained by exploiting the temperature glide effect. How large savings that can be achieved in practice depends on mixing the right refrigerants at the right mixing ratio.

This research project is financially supported by the Danish Energy Agency's EUDP programme (Energy Technology Development and Demonstration).

Project number: 64016-0045.

The project is carried out in cooperation with the Technical University of Denmark and the following industrial cooperating partners: Alfa Laval, Sauter and danARCTICA.

The following persons have participated in the project:

- Rolf Christensen, Alfa Laval
- Mads Munck Jakobsen, Sauter
- Jan Larsen, danARCTICA
- Brian Elmegaard, Technical University of Denmark
- Wiebke Brix Markussen, Technical University of Denmark
- Jonas Kjær Jensen, Technical University of Denmark
- Claus Madsen, Danish Technological Institute
- Cristopher Murphy, Danish Technological Institute
- Jóhannes Kristófersson, Danish Technological Institute
- Benjamin Zühlsdorf, Danish Technological Institute
- Lars Olsen, Danish Technological Institute

The project team would like to thank the EUPD programme (Danish Energy Agency) for supporting the project with valuable inspiration.

1.1. Project Details

Project title	Mixed refrigerant heat pumps/ cooling systems (MIREHP)
Project identification (program abbrev. and file)	EUDP 2016, Project no.: 64016-0045
Name of the programme which has funded the project	Energiteknologisk Udviklings- og Demonstrationsprogram (EUDP)
Project managing company/institution (name and address)	Danish Technological Institute, Gregersensvej 1, DK-2630 Taastrup
Project partners	Alfa Laval Sauter danARCTICA Technical University of Denmark
CVR (central business register)	56976116
Date for submission	15 October 2019

1.2. Short Description of Objectives and Results

English version

The aim of the project is to develop a new heat pump concept using zeotropic refrigerant mixtures as working medium which can provide a significant boost in system efficiency. If an appropriate temperature match is obtained between the refrigerant and brine, a considerable COP enhancement can be obtained by exploiting the temperature glide effect.

Several system designs have been evaluated through a series of simulations with different refrigerant mixtures of natural refrigerants. The most promising system design from the simulations has been built and tested. A test heat pump has been built by danARCTICA, and tests have been performed and analyzed.

The tests have shown an efficiency improvement of 15 % by a combination of propane with CO_2 and by using a suction gas exchanger. The simulations show that it is possible to obtain an even higher performance improvement with other temperatures and mixtures.

Danish version

Formålet med projektet er at udvikle et nyt varmepumpekoncept ved brug af zeotropiske kølemiddelblandinger som arbejdsmedium for at opnå en signifikant forbedring af systemeffektiviteten. Hvis der er et passende temperaturmatch mellem kølemidlet og brinen, kan der opnås en betydelig COP-forbedring ved at udnytte effekten af temperaturglidet.

Flere systemopbygninger er blevet evalueret gennem en række simuleringer med forskellige kølemiddelblandinger af naturlige kølemidler. Den mest lovende systemopbygning fra simuleringerne er blevet bygget og testet. En testvarmepumpe er blevet bygget ved danARCTICA, og tests er blevet udført og analyseret.

Testene viste en effektivitetsforbedring på 15 % ved brug af stofparret propan / CO_2 og ved brug af sugegasvekslere. Simuleringerne viste, at det er muligt at opnå en endnu større effektivitetsforbedring med andre temperatursæt og kølemidler.

1.3. Executive Summary

English

By using mixtures of natural refrigerants in refrigeration systems and heat pumps, a better system efficiency can be achieved resulting in energy savings, especially in processes with a large temperature glide.

Already today, hybrid absorption/compression heat pumps using an ammonia/water mixture as refrigerant are in use. The process used in typical hybrid absorption/ compression heat pumps has a large, and more or less the same temperature glide on both the evaporator and condenser side of the heat pump.

A greater range of system configurations for mixtures has been simulated and compared with results from the hybrid absorption / compression process by various combinations of temperature changes of the source and sink. One of the intentions is to find the optimal configuration for use in cases with different temperature changes and temperature differences on the source and sink side.

If an appropriate temperature match is established between the refrigerant and the brine, and if, at the same time, a sufficient heat exchanger area is used, and if suction gas exchangers are used for the superheating itself, then a significant COP improvement can be achieved by utilizing the effect of the temperature glide in a relatively simple plant. The amount of savings that can be achieved depends on the refrigerant chosen and on the choice of mixing ratio.

The theory underlying the project has required specialized expertise, testing and optimization of refrigerant mixtures as well as the development of and testing on a pilot setup. To ensure adequate knowledge, skills and practical expertise, a project team has been composed with participants from DTU, Danish Technological Institute (DTI), danARCTICA, Sauter, and Alfa Laval. Together, they represent some of Denmark's best people within research, theoretical knowledge, project management, and practical experience.

Simulations have shown an improved efficiency of up to 27 % depending on the selected temperature set and mixture used. The work has shown that it was possible to achieve an efficiency improvement of 15 % with a simple cooling circuit with integrated subcooler and suction gas exchanger. The refrigerant mixture CO_2 / propane was chosen for the test.

Danish

Ved at benytte blandinger af naturlige kølemidler i kølesystemer og varmepumper kan der realiseres en bedre systemeffektivitet med deraf følgende energibesparelser. Dette er især relevant i processer, hvor der forekommer store temperaturglid.

Allerede i dag anvendes der nogle steder hybride absorptions-/kompressionsvarmepumper med en blanding af ammoniak og vand som kølemiddel. Den typiske hybride absorptions-/kompressionsvarmepumpe har et stort, og mere eller mindre det samme temperaturglid på både fordamper- og kondensatorsiden.

En større vifte af systemkonfigurationer til blandinger er blevet simuleret og sammenlignet med resultater fra hybrid absorptions-/kompressionsprocessen ved forskellige kombinationer af temperaturændringer på kilde- og drænsiden. Hensigten har blandt andet været at finde den optimale konfiguration, hvis der er forskellige temperaturændringer og temperaturdifferencer på kilde- og drænsiden.

Hvis der etableres et passende temperaturmatch mellem kølemidlet og brinen, og der samtidig anvendes et tilstrækkeligt varmevekslerareal, og der gøres brug af sugegas-vekslere til selve overhedningen, så kan der opnås en betydelig COP-forbedring ved at udnytte effekten af temperaturglidet i et relativt simpelt anlæg. Hvor stor en besparelse, der kan opnås, afhænger af valget af kølemiddel og blandingsforhold.

Teorien, som ligger til grund for projektet, har krævet en specialiseret ekspertviden, afprøvning og optimering af kølemiddelblandinger såvel som udvikling af og funktionel analyse på et pilottestanlæg. For at sikre tilstrækkelig viden, knowhow og praktisk ekspertise er et projektteam derfor blevet sammensat med deltagere fra DTU, Teknologisk Institut, danARCTICA, Sauter og Alfa Laval. Disse repræsenterer tilsammen nogle af landets største kompetencer inden for forskning, teoretisk viden, projektledelse og praktisk erfaring.

Simuleringer viste en forbedret effektivitet på op til 27 % alt afhængigt af det valgte temperatursæt og den anvendte blanding. Arbejdet har vist, at det var muligt at opnå en effektivitetsforbedring på 15 % med en simpel kølekreds med integreret underkøler og sugegasvekslere. Stofparret CO_2/propan blev udvalgt og anvendt i testopstillingen.

1.4. Project Objectives

The aim of the project has been to collect and develop knowledge in the area of refrigerants in order to find the best suitable zeotropic mixtures as well as to build a pilot setup for conducting functional analysis to validate the theoretical foundation and gain experience regarding an optimal setup configuration and control of the system.

The result is an improved overall performance for many applications with a large temperature glide.

The objective is achieved by carrying out research on how the different mixtures are combined most optimally through gained experience from the testing of the concept as well as by calculating the expected performance.

1.5. Project Results, Dissemination and Utilization of Results

In the project, the MIREHP concept is elaborated by carrying out research encompassing both calculation of the performance and experimental work with different mixture configurations. Also, a calculation tool has been developed.

The objectives stated in the project proposal have been obtained by the conducted research, which shows that the technology is feasible for the intended purposes.

A large number of simulations have been carried out on various potential system configurations for the use of mixtures of natural refrigerants. A test setup has been built whose purpose was to document the benefits of using mixtures. A control system has been built with an associated data acquisition system, so it was possible to operate the heat pump for the purpose and to be able to document the expected COP.

The expected efficiency improvement was 10 to 30 %. Simulations have shown maximum improvement of as much as 27 %, depending on the selected temperature set and mixture. The work has shown that it is possible to achieve an efficiency improvement of 15 % by using the refrigerant mixture CO_2 / propane and by using suction gas heat exchangers at typical conditions.

The application described two system configurations, one simple and one advanced. Both were among those simulated in the project. The simple one turned out to be the preferred configuration why only this one was built and tested.

The test setup was not built for the purpose that the system could be used directly as a final design. The system should only be able to document that the concept worked, which it has been able to do, but a commercial product optimized for individual tasks still remains.

In order to achieve a sustainable commercial product, the following tasks have to be elaborated:

- An optimized / simplified plant design based on the concept, and still maintaining the large COP.
- Make the system design less expensive for combustible mixtures in relation to the ATEX directive and perhaps make a design to completely avoid any leakage to be combustible.
- Envisage a method that can detect if the mixture composition has changed.
- Investigate the sensitivity of the COP for different mixtures with variations of temperature differences of the water for both the source and sink side.

1.6. Utilization of Project Results

The results obtained in the project have documented the potential stated in the application. However, as indicated in section 1.5, there are still several issues which remain to be solved and developed before a final design of the heat pump is completed.

The benefits of using a suction gas heat exchanger, which can also compensate for an undesirable and uneven distribution in the evaporator, can also be transferred to applications with pure refrigerants, in addition to the corresponding result in increased COP

during part load, as in the case of mixtures, if the water flow is maintained through the evaporator.

1.7. Project Conclusion and Perspective

The primary purpose of the project has been to provide an understanding of the advantages of using the mixed refrigerant concept in heat pumps. In addition, the focus has been on optimizing the selection and the mixing properties of the refrigerants.

The concept of using mixtures and the benefits of using them have been demonstrated in the project. A theoretical study has been made of which mixtures that can be advantageously used with selected temperature sets in different system configurations, and which efficiency improvements that can be achieved.

Measurements have been carried out on the test set-up with the propane-CO_2 mixture, which has demonstrated the concept of using a suction gas heat exchanger, and the results have fulfilled the expected potential.

The prospects are great because it has been possible to use mixtures of natural refrigerants which are also future-proofed. And the final system design, which was also the simplest of all investigated, also proved to be the one that in the vast majority of cases also generated the highest COP. At the same time, it has been demonstrated that the concept can also compete with regard to the COP compared to existing solutions. In the long term, it will also be possible to raise the concept to a level where it will be competitive on price.

It is extremely interesting that it has been possible to obtain a COP with mixtures that are higher than similar systems with the refrigerant ammonia, because a heat pump based on mixtures can be built of components that are far cheaper than ammonia related components. In order to generate the same COP for heat pumps with ammonia as with mixtures, one would have to install a number of heat pumps in series, which is just more expensive than just a single unit in double size. With mixtures, the system can operate with relatively large temperature differences between the outlet temperatures at the two sides using only a 1-stage system, compared to what can be operated with an ammonia system. When using an ammonia-based plant, the designer is often forced into a two-stage system due to a high-pressure gas temperature.

With the large focus on the integration of heat pumps in general, heat pumps based on mixtures could play a significant role in that relationship.

2. Introduction

In this project, the aim has been to develop a new heat pump concept using zeotropic refrigerant mixtures as working medium. By using zeotropic mixtures, a significant boost in system efficiency is achieved. See the table below for efficiency gain for different applications.

A zeotropic mixture is a refrigerant mixture that never has the same vapor phase and liquid phase composition at the vapor–liquid equilibrium state. The interest in using zeotropic refrigerant mixtures is due to the energy saving, which theoretically can be obtained by using a Lorenz based process instead of a Carnot process. The Lorenz process describes a

thermodynamic cycle using zeotropic mixtures, while the Carnot process describes pure single component refrigerants.

If an appropriate temperature match is obtained between the refrigerant and brine, and a sufficient heat exchange area is used, a considerable COP enhancement can be obtained by exploiting the temperature glide effect.

How large savings that can be achieved in practice depends on mixing the right refrigerants at the right mixing ratio. The work has been constrained to only mixtures of components that provide the best possible protection of the environment, i.e. natural refrigerants.

The reason why zeotropic mixtures still have not been implemented to a larger extent despite many years of knowledge of the advantages thereof can probably be explained by that the large savings will only be achieved if the temperature lift is relatively large.

Previous research in zeotropic mixtures was based on phasing out the refrigerants R22 and R12 associated with cooling systems, and in these cases, the energy benefits related to the relatively small temperature lifts were limited. The total benefit has been reduced by the lower heat transfer coefficient with zeotropic mixtures.

The interest in heat pumps with large temperature lifts has increased the last 10 years, and the development has now reached a stage where mixes of refrigerants will be the most obvious possibility to improve the efficiency significantly.

The hybrid process is relatively new and is characterized by always operating with the same concentration through the evaporator and the condenser, which results in a uniform temperature glide of the refrigerant in both the evaporator and the condenser.

3. Final Scientific Dissemination of the Research in the MIREHP Project

3.1. Introduction

The MIREHP project seeks to identify possible performance enhancement measures for industrial heat pumps by utilizing zeotropic mixtures and advanced heat pump cycle configurations. The use of zeotropic mixtures can theoretically reduce the heat transfer irreversibilities by matching the condensation and evaporation temperature profiles to the temperature profiles of the sink and source.

The project has a special emphasis on challenging heat pump operating conditions mainly those in which there is a significant difference between the temperature profile of the heat sink and the heat source. Under these operating conditions, it may be difficult to attain a good profile match in both the heat sink and heat source simultaneously when using a simple heat pump cycle configuration. Consequently, the best coefficient of performance (COP) is attained when the best trade-off between matching the sink or source profiles is attained. In these cases, there may thus still be a significant reduction of COP due to heat transfer irreversibilities and hence a potential to increase the performance if the glide match could be controlled better.

Some advanced cycle configurations such as the hybrid absorption compression heat pump (HACHP) offers additional degrees of freedom, which can be used to attain a better glide match in the process. This is generally attained by implementing internal liquid circulation, which can be used to control vapour quality or concentration at different locations in the process, subsequently altering the temperature profiles during phase change.

The present work presents results for a numerical analysis, which seeks to compare the performance of a range of cycle configurations under a number of more or less challenging operating conditions. The comparison is further subjected to a range working fluid mixtures and compositions.

The work performed in the MIREHP project is divided into two subtasks. Initially, a screening for refrigerant mixtures was performed for the simplest cycle configuration under varying boundary conditions and cycle characteristics. This analysis seeks to reveal the improvement potential by applying zeotropic mixtures in simple cycle heat pumps. Further, the analysis seeks to identify the sources of irreversibility that prevail in the improved simple cycles with zeotropic mixtures. This will allow us to identify possible advanced cycle configurations capable of alleviating the prevailing sources of irreversibilities.

The identification of possible advanced cycle configurations leads to the second subtask of the MIREHP project: Evaluation of advanced cycles configurations and refrigerant mixture screening for these cycles.

In this report the applied methodology and the derived results are presented individually for the two subtasks.

3.2. Subtask 1: Simple Cycle Refrigerant Screening

3.2.1. Methods

In order to analyse the potential improvement attained by the use of zeotropic mixtures, different cases with different boundary conditions were defined, representing a range of possible applications. For this study, it was assumed, that the heat source consists of a stream with a temperature of 40 °C, which is a representative value for industrial excess heat temperatures. The source is used to heat another stream from 40 °C to 80 °C, which is within a common temperature range for industrial low temperature processes. The outlet temperature of the heat source is not fixed and will be varied in the cases as shown in Table 1.

Table 1: Definition of boundary conditions for considered cases.

Case Number	Heat Source $T_{\text{source,in}} \rightarrow T_{\text{source,out}}$	Heat Sink $T_{\text{sink,in}} \rightarrow T_{\text{sink,out}}$
I	40 °C → 35 °C	40 °C → 80 °C
II	40 °C → 30 °C	
III	40 °C → 25 °C	
IV	40 °C → 20 °C	

These four cases could be representative of both a booster heat pump for a low temperature district heating network or an industrial application in which an excess heat stream of a process can be exploited in a heat pump to heat another process stream to a useable temperature. The variation in heat source outlet temperature can be seen as a variation of the available capacity of the heat source. The higher the available capacity is the higher the heat source outlet temperature will be. High heat source capacities are for instance attained when latent heat from condensation of moist air is recovered.

3.2.2. Heat Pump Model

3.2.2.1. Thermodynamic Model

The heat pump model was implemented for a simple vapor compression cycle as shown in Figure 1. It consists of the minimum number of required components and represents the simplest possible heat pump solution. Therefore, the analysis focused solely on the influence gained from using mixtures and included the possibility to derive recommendations for possible adjustments of the cycle layout.

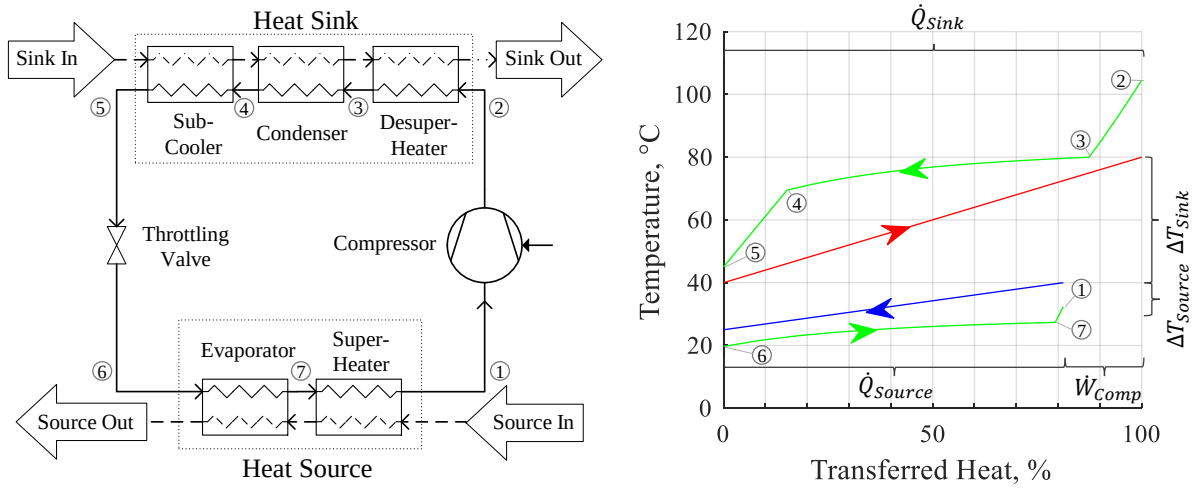

Figure 1: Flow chart of modelled heat pump (left) and diagram with temperature profiles over transferred heat for case II with 10 % CO_2 – 90 % DME (dimethylether) as working fluid (right).

The heat pump process described a working fluid which receives heat from the heat source at low pressure (6 → 1), before it is compressed to a higher pressure (1 → 2) in order to reject heat to the heat sink at high temperatures (2 → 5), before it is expanded to the low pressure again (5 → 6). The heat rejection can occur subcritically or supercritically, while the low pressure side is always below the critical point.

The model was based on the First and Second Law of Thermodynamics and includes energy and mass balances for all components. The heat exchangers were modelled as separate control volumes according to single-phase and two-phase flow, disregarding if they are manufactured as one component. This distinction diminishes for transcritical processes, which was for numerical reasons assumed at pressures above 95 % of the critical pressure. The heat exchangers implying phase change are discretized in steps of equal amounts of transferred heat along the flow direction to enable the calculation of temperature profiles during the phase change. A discretization in 15 state points for the condenser and 10 for the evaporator was found to provide sufficient accuracy with an acceptable tolerance.

In order to calculate the condensation and evaporation pressure a minimum pinch point temperature difference of $\Delta T_{\mathrm{pinch,min}} = 5\ \mathrm{K}$ was introduced. The possible performance gain from subcooling is always completely exploited by defining the temperature at point 5 (T_5) by the pinch point temperature difference above the sink inlet temperature. While fixing the condensation pressure by setting the minimum temperature difference to the minimum required pinch temperature difference yields the maximum COP for subcritical processes, this may not always be applicable for transcritical processes. The pressure has therefore been optimized for transcritical pressures with respect to COP considering a boundary on the minimum temperature difference, which corresponds to defining the pressure by the pinch point temperature difference. It may be noted, that the optimal gas cooler pressure resulted only in very exceptional cases in a minimum temperature difference larger than the minimum required pinch point temperature difference.

The compression process was modelled with an isentropic efficiency of $\eta_{\mathrm{comp,is}} = 0.8$ while losses from the electrical motor to the environment were disregarded. The volumetric heating capacity VHC relates the supplied heat load to the volume flow rate at the inlet of

the compressor and indicates the size of the component. In order to protect the compressor from wet compression a minimum superheating temperature difference of $\Delta T_{\mathrm{SH}} = 5\ \mathrm{K}$ is considered at both inlet and outlet of the compressor. For additional analyses of the influence of the superheating on the COP the simulations were repeated without superheating.

The throttling process was assumed to be isenthalpic.

The model was implemented in Matlab and used medium properties from Refprop with the recommended state of the art models for the equations of state and mixing parameters for all modelled fluid mixtures.

3.2.2.2. Exergy Analysis

In order to identify the inefficiencies in the systems an exergy analysis was conducted. The exergy flow rates $\dot{E}$ were calculated for the mass flows at each state point as well as for the consumed power. The dead state was defined as $T_0 = 25\ °\mathrm{C}$ and $p_0 = 1\ \mathrm{bar}$. The exergy destruction $\dot{E}_D$ was defined as the difference between all exergy flows entering and leaving a control volume, which is equivalent to the difference between the exergy fuel $\dot{E}_F$ and exergy product $\dot{E}_P$. The exergy fuel and product were defined as the desired and invested exergetic effect and therefore dependent on the function of the component. For dissipative components, such as the throttling valve, no meaningful definition of the product can be found.

$$\dot{E}_D = \dot{E}_F - \dot{E}_P = \sum_{i=1\ldots k} \dot{E}_i \tag{1}$$

The exergy destruction describes the irreversibilities within the components as an absolute value. Since the absolute energy flows in the different components can vary, the exergy destruction varies as well and is therefore not an optimal measure for comparisons of performance. A supplementing indicator is the exergy efficiency, defined as the ratio of the exergetic product over the exergetic fuel.

Nevertheless, it can hardly be used to analyse the improvement potentials, since it determines the overall exergy destruction by an outer balance equation, rather than locating the origin of the irreversibilities within the component. It does furthermore not contain information about whether the exergy destruction could be avoided by e.g. an optimal mixture having a constant temperature difference along the transferred heat.

Therefore, we suggested to distinguish between two contributions as shown in Figure 2, i.e., exergy destruction $\dot{E}_{D,\mathrm{pinch}}$ which is caused by the nature of the component having a finite heat transfer area and cannot be avoided even with an ideal fluid and an additional exergy destruction $\dot{E}_{D,\mathrm{fluid}}$ which accounts for real working fluid being non-ideal. The sum of the exergy destruction from both contributions yield the total exergy destruction occurring within the component $\dot{E}_{D,\mathrm{component}}$.

$$\dot{E}_{\mathrm{D,component}} = \dot{E}_{\mathrm{D,pinch}} + \dot{E}_{\mathrm{D,fluid}} \tag{2}$$

If the heat exchanger is assumed to be an ideal component with an infinite heat exchanger area, the exergy destruction related to the pinch $\dot{E}_{D,\text{pinch}}$ would diminish, but the exergy destruction accounting for the difference between a real and an ideal fluid $\dot{E}_{D,\text{fluid}}$ would still contribute to the total component exergy destruction.

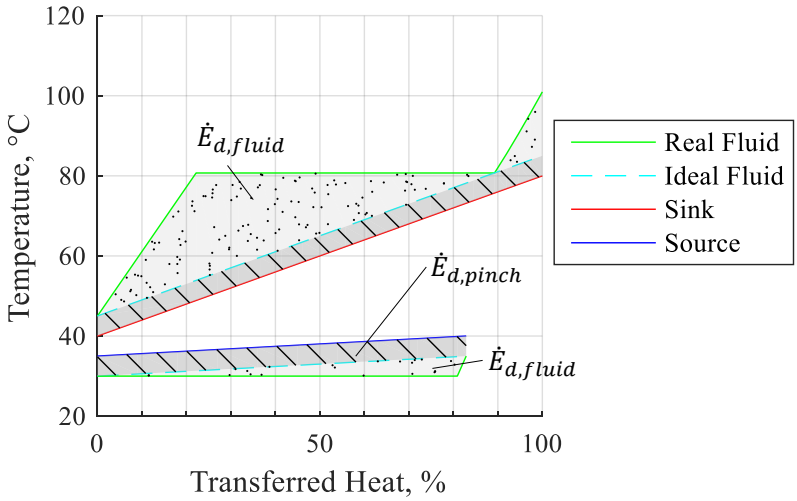

Figure 2: Diagram with temperature profiles over transferred heat with exergy destruction highlighted.

The exergy destruction accounting for the minimum temperature difference can be determined by an exergy balance between the ideal fluid and the sink or source stream accordingly. In order to calculate the exergy flow $\dot{E}_Q$ of a heat flow rate $\dot{Q}$ which is rejected or received with a constant capacity rate between the temperatures T_1 and T_2, the thermodynamic average temperature $\bar{T}_{1-2} = (T_1 - T_2)/\ln(T_1/T_2)$ is introduced. Using this relation, the exergy balance defines the exergy destruction as:

$$\dot{E}_{\text{D,pinch}} = \left(1 - \frac{T_0}{\bar{T}_{\text{hot}}}\right)\dot{Q} - \left(1 - \frac{T_0}{\bar{T}_{\text{cold}}}\right)\dot{Q} = T_0\,\dot{Q}\,\frac{\bar{T}_{\text{hot}} - \bar{T}_{\text{cold}}}{\bar{T}_{\text{hot}}\,\bar{T}_{\text{cold}}} \tag{3}$$

The indices "hot" and "cold" refer to the ideal fluid during condensation and the heat sink stream in the sink heat exchanger and in the heat source heat exchanger to the heat source stream and the ideal fluid during evaporation, respectively.

Using Equation 3 and the definition of the thermodynamic average temperature for streams with a constant heat capacity, the exergy destruction in sink and source due to the pinch point temperature difference ΔT_{pinch} can be directly expressed as a function of this temperature difference:

$$\dot{E}_{\text{D,pinch,source}} = T_0\,\dot{Q}_{\text{source}}\,\frac{1}{T_{\text{source,in}} - T_{\text{source,out}}}\ln\left(\frac{T_{\text{source,out}}}{T_{\text{source,in}}}\left(\frac{T_{\text{source,in}} - \Delta T_{\text{pinch}}}{T_{\text{source,out}} - \Delta T_{\text{pinch}}}\right)\right) \tag{4}$$

$$\dot{E}_{\text{D,pinch,sink}} = T_0\,\dot{Q}_{sink}\,\frac{1}{T_{\text{sink,out}} - T_{\text{sink,in}}}\ln\left(\frac{T_{\text{sink,out}}}{T_{\text{sink,in}}}\left(\frac{T_{\text{sink,in}} + \Delta T_{\text{pinch}}}{T_{\text{sink,out}} + \Delta T_{\text{pinch}}}\right)\right) \tag{5}$$

As an indicator to describe the match of the temperature profiles we introduce the temperature matching indicator π_{glide} as the ratio of the total exergy destruction $\dot{E}_{D,\text{component}}$ over $\dot{E}_{D,\text{pinch}}$:

$$\pi_{\text{glide}} = \frac{\dot{E}_{\text{D,component}}}{\dot{E}_{\text{D,pinch}}} = \frac{\dot{E}_{\text{D,fluid}} + \dot{E}_{\text{D,pinch}}}{\dot{E}_{\text{D,pinch}}} \tag{6}$$

For an optimal match of the temperature profiles the matching indicator will approach $\pi_{\text{glide}} = 1$ whereas it increases with an increasing mismatch.

This definition enables additionally to determine the share of exergy destruction caused by the fluid being non-ideal on the entire exergy destruction of the system $y^*_{\text{D,fluid}}$ and thereby represents the potential decrease in exergy destruction by finding an optimal fluid:

$$y^*_{\text{D,fluid}} = \frac{\dot{E}_{\text{D,fluid}}}{\dot{E}_{\text{D,total}}} \tag{7}$$

The factor can be used to analyse the potential performance increase that can be obtained by better matching the temperature profiles in either sink or source, e.g. $y^*_{\text{D,fluid,source}} = \dot{E}_{\text{D,fluid,source}}/\dot{E}_{\text{D,total}}$, or to highlight the total potential reduction of exergy destruction $y^*_{\text{D,fluid,total}} = \left(\dot{E}_{\text{D,fluid,source}} + \dot{E}_{\text{D,fluid,sink}}\right)/\dot{E}_{\text{D,total}}$.

The introduced distinction between exergy destruction which could potentially be avoided by finding an optimal fluid and exergy destruction resulting from component inefficiencies cannot be applied to the compression and expansion process, since these processes convert mechanical work into internal energy, which can theoretically be reversible for any fluid. In these cases, properties of the real fluids do not cause any additional exergy destruction.

3.2.2.3. Refrigerant Screening

The list of fluids which were considered in the design of the binary mixtures can be defined according to different aspects. No strong correlation could be observed in a previous study, which relates specific medium properties to the performance of a heat pump, when using the fluid as a component in a working fluid mixture. It therefore seemed promising to assemble the group of pure fluids for designing the mixtures with fluids covering a broad range of typically relevant medium characteristics, such as the normal boiling point and the critical point. Considering the possibility to use mixed working fluids enlarges the variety of working fluids substantially compared to a limited set of pure fluids. This obviates the need to consider fluids with unfavourable characteristics such as high ODP or GWP.

Based on this, the group of commonly used natural refrigerants and the two higher boiling HCs, n-Hexane and Heptane, are chosen for this study as shown in Table 2. The natural refrigerants entail a good and low-cost availability, limited toxicity, low environmental impact and good miscibility among each other, while being established working fluids.

Table 2: List of fluids considered in the design of binary mixtures above dashed line and additionally considered fluids below dashed line.

No.	Name of Fluid	Ref. No.:	Type	ODP, -	GWP, -	Normal Boiling Point, °C	Crit. Temp., °C	Crit. Pres., bar	Safety Class
1	Methane	R-50	HC	0	25	-161.5	-82.6	46.0	A3
2	Ethylene	R-1250	HO	0	6.8	-103.8	9.2	50.4	A3
3	Ethane	R-170	HC	0	2.9	-88.6	32.2	48.7	A3
4	CO_2	R-744		0	1.0	-	31.0	73.8	A1
5	Propylene	R-1270	HO	0	3.1	-47.6	91.1	46.7	A3
6	Propane	R-290	HC	0	3.0	-42.0	96.7	42.5	A3
7	Dimethylether (DME)	R-E170	HC	0	1.0	-24.0	127.3	53.4	A3
8	Iso-Butane	R-600a	HC	0	3.0	-11.7	134.7	36.3	A3
9	n-Butane	R-600	HC	0	3.0	-0.5	152.0	38.0	A3
10	Iso-Pentane	R-601a	HC	0	4.0	27.8	187.3	33.8	A3
11	Ethylether (DEE)	R-610	HC	0	4.0	34.6	193.7	36.4	A3
12	Pentane	R-601	HC	0	4.0	36.1	196.6	33.7	A3
13	n-Hexane		HC	-	-	68.7	234.5	30.3	-
14	Heptane		HC	-	-	98.4	267.0	27.4	-
15	Ammonia	R-717		0	0.0	-33.3	132.4	112.8	B2
16	Water	R-718		0	0.2	100.0	373.9	220.6	A1

The miscibility has been analysed using a group contribution method. Immiscibility of the fluids would result in two liquid phases with different compositions, so called miscibility gaps, which could have unfavourable influences on the operation. The fluids above the dashed line in Table 2 are widely miscible with each other with minor miscibility gaps in the mixtures including ethers. Especially mixtures with DME have miscibility gaps, whereas DEE shows good miscibility with the other fluids. The ethers are fully miscible. The miscibility of the fluids above the dashed line with water and ammonia is limited over the complete required range of pressure and temperature. Based on this, all possible binary mixtures among the fluids 1 to 14 and among water and ammonia are considered in the study. In case a mixture including the ethers appears to be a promising solution, further analysis with respect to the miscibility is required.

The increased flammability of the natural refrigerants is accepted, since it is assumed that technically and economically feasible solutions exist. Furthermore, R290 and R600a are commonly used in commercial products and considered suitable for industrial applications.

The model was evaluated for all pure components and all possible binary mixtures at 9 compositions resulting from the fluids in Table 2. This procedure produced a comprehensive set of 833 thermodynamic cycle simulations per case which is used as a basis for analysing the relation between the temperature glide matches and the performance.

3.2.3. Results

Figure 3 gives an overview of the calculated COP of the heat pump for all possible mixture combinations for cases I to IV and Table 3 presents an overview of the best performing pure and mixed working fluids for each case. All four cases assumed the same supply temperature by heating water from 40 °C to 80 °C and the same heat source inlet temperature of 40 °C, while case I was defined by cooling down the heat source by a temperature difference of 5 K, which increased stepwise to 20 K for case IV. Each line represents the COP of one binary mixture with a composition varying from zero to one for the less volatile component x_2. For some cases, no technically feasible results were obtained, e.g. because the evaporation process is transcritical due to a too low critical temperature. These points are not included and cause discontinuities in some curves.

The maximum achievable COP decreased from case I to IV with an increasing source temperature glide and thereby a lower mean temperature in the heat source. The obtained COPs decreased accordingly, whereas additional analysis showed that the best exergetic efficiencies for all four cases were in the range of 50 % to 52 %.

It can be seen in Figure 3 and Table 3 that the performance is increased when mixtures are used with a large temperature glide in the heat source. For case I, the best performance was obtained by pure working fluids while case IV showed a significant increase in COP by using mixed working fluids.

Propylene, DME and Propane showed the best performance in case I with a COP between 5.85 and 5.82. The glide matching indicator for the source π_{so} was between 1.53 and 1.54 whereas the sink showed a higher mismatch.

Case II assumes a temperature glide of 10 K in the source stream, which caused an increased mismatch in the source for the pure fluids. DME and Propylene have values of $\pi_{so} = 2.05$, while the temperature glide can be approached better by mixtures. The two best mixtures 10 % CO_2 – 90 % DME and 50 % DME – 50 % Butane have a source temperature glide match of 1.56 and 1.59, respectively. The maximum COP obtained from the mixtures is 5.62, which is equal to an increase of 6.4 % when compared to the COP of the best pure fluid of 5.28.

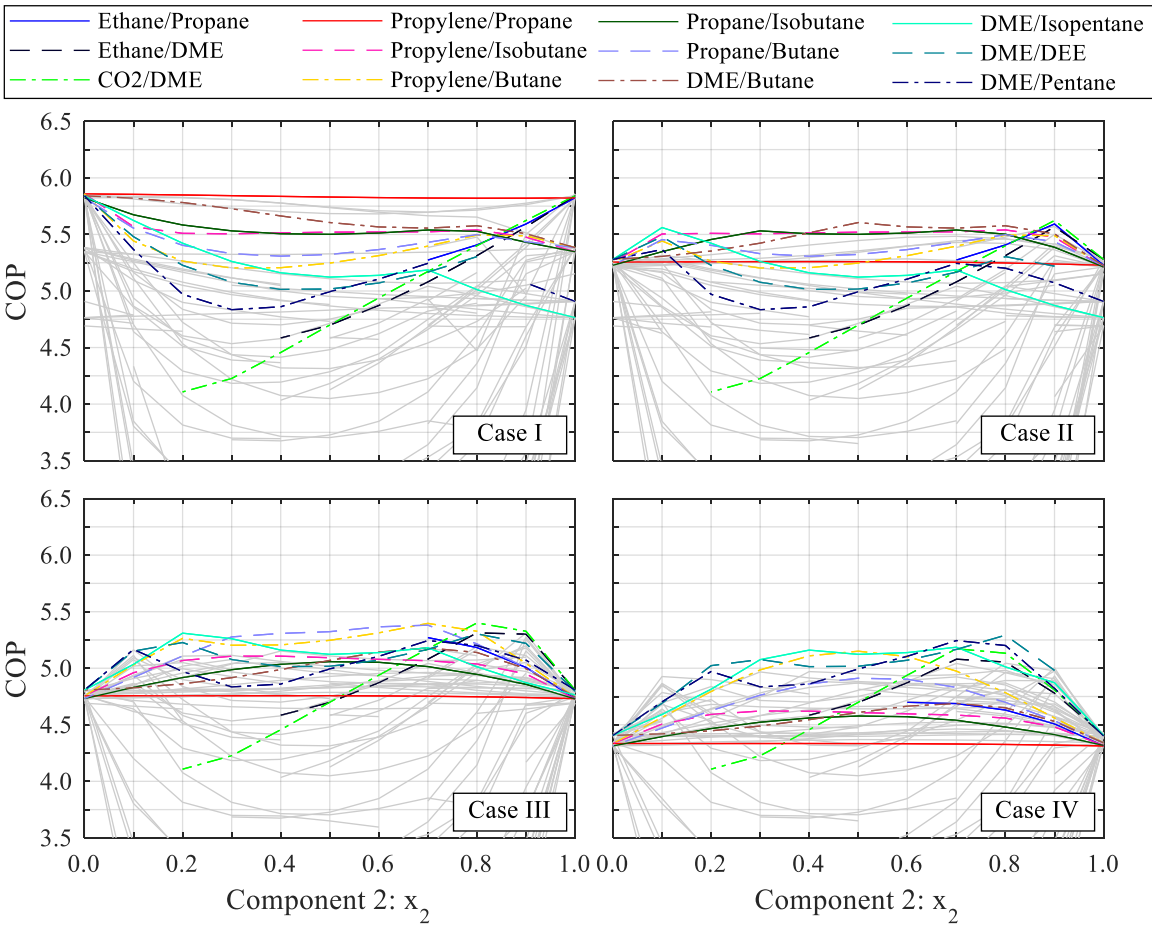

Figure 3: COP for all cases with minimum 5 K superheating for all mixtures over the composition of the less volatile component 2. Selected mixtures are labelled while other mixtures are included as grey shaded, representing the general solution space.

The performance gain from using mixtures reached 12 % for case III and 20 % for case IV. The simulations without superheating have shown an increase in COP from 4.38 to 5.56 which corresponds to 27 % for Case IV. The values for the temperature glide match indicator in the source are around 1.5 for the best mixtures in Case III and IV while for the pure fluid they are approximately 2.5 for case III and 3.0 for case IV. The temperature glide match indicators in the sink were for the best solutions in case III below 3.0 and in case IV below 2.5, whereas the mismatch for the best pure fluids was in both cases larger than 3.5.

The pressure ratios of the presented best cases were mostly below 4 for moderate absolute pressures which can be assumed as technologically feasible. The volumetric heating capacities VHC vary between 700 kJ/m^3 for fluids with low evaporation pressures and reaches up to more than 10,000 kJ/m^3 for higher evaporation pressures, indicating a relatively high heat supply rate with compact compression equipment.

Table 3: Simulation results for best performing mixtures and pure fluids for each case and a minimum of 5 K superheating.

Medium	COP	π_{so} -	π_{si} -	p_{ev} bar	p_{co} bar	VHC kJ/m³
Case I						
Propylene	5.85	1.53	2.80	13.1	35.7	9,508
DME	5.84	1.54	3.43	6.8	22.6	6,106
Propane	5.82	1.53	2.92	10.8	31.1	8,093
Butane	5.38	2.24	3.61	2.5	11.0	2,512
Isobutane	5.34	2.28	3.48	3.6	14.4	3,308
Pentane	4.91	3.34	3.74	0.6	4.1	721
Case II						
10 % CO_2 – 90 % DME	5.62	1.56	2.96	7.5	25.1	6,564
50 % DME – 50 % Butane	5.61	1.59	3.14	4.8	17.3	4,329
10 % Ethane – 90 % Propane	5.60	1.42	2.58	12.3	35.9	8,761
10 % Ethane – 90 % Propylene	5.57	1.48	2.50	14.5	39.5	10,060
DME	5.28	2.05	3.42	5.9	22.5	5,368
Propylene	5.26	2.05	2.80	11.5	35.5	8,467
Case III						
30 % Propylene – 70 % Butane	5.40	1.47	2.84	4.0	15.0	3,573
30 % Propane – 70 % Butane	5.38	1.42	2.98	3.9	14.8	3,475
10 % CO_2 – 90 % DME	5.32	1.56	2.97	7.0	25.0	6,138
80 % DME – 20 % Isopentane	5.31	1.89	2.87	4.5	17.2	4,112
Pentane	4.81	2.48	3.74	0.6	4.1	693
DME	4.80	2.58	3.42	5.1	22.3	4,701
Case IV						
20 % DME – 80 % DEE	5.29	1.33	2.47	1.2	6.1	1,312
30 % DME – 70 % Pentane	5.24	1.62	2.00	1.2	6.1	1,330
30 % DME – 70 % Isopentane	5.19	1.74	2.20	1.7	8.0	1,757
50 % Propylene – 50 % Butane	5.15	1.52	2.56	5.0	18.6	4,270
Isopentane	4.41	2.98	3.69	0.6	5.0	747
DME	4.41	3.10	3.42	4.4	22.2	4,101

The good temperature glide in the evaporator for the pure fluids stemmed from the source temperature glide of 5 K and the minimum required superheating of 5 K. This caused the pinch point temperature difference to be located at both the inlet and outlet of the heat source and thus, a good temperature match. In some cases, the superheating by the heat source can be avoided by using e.g. an internal heat exchanger. The same set of simulations was therefore repeated for zero superheating as shown in Figure 4. It may be noted that the results for the cases without superheating of 5 K correspond relative well to the cases with 5 K higher temperature glide in the source.

The water ammonia mixtures did not show competitive COPs. The mixtures have a high and nonlinear temperature glide which resulted in a high mismatch on at least one side. All solutions showed unfavourable operation conditions such as very high compressor discharge temperatures for a high share of water and high compressor discharge temperatures and high pressures for an increasing share of ammonia.

Figure 5 shows the performance of all solutions for case I to IV over the glide matching indicators for sink and source. In order to allow comparisons between the cases with a different maximum achievable COP the exergetic efficiency was chosen to indicate the performance.

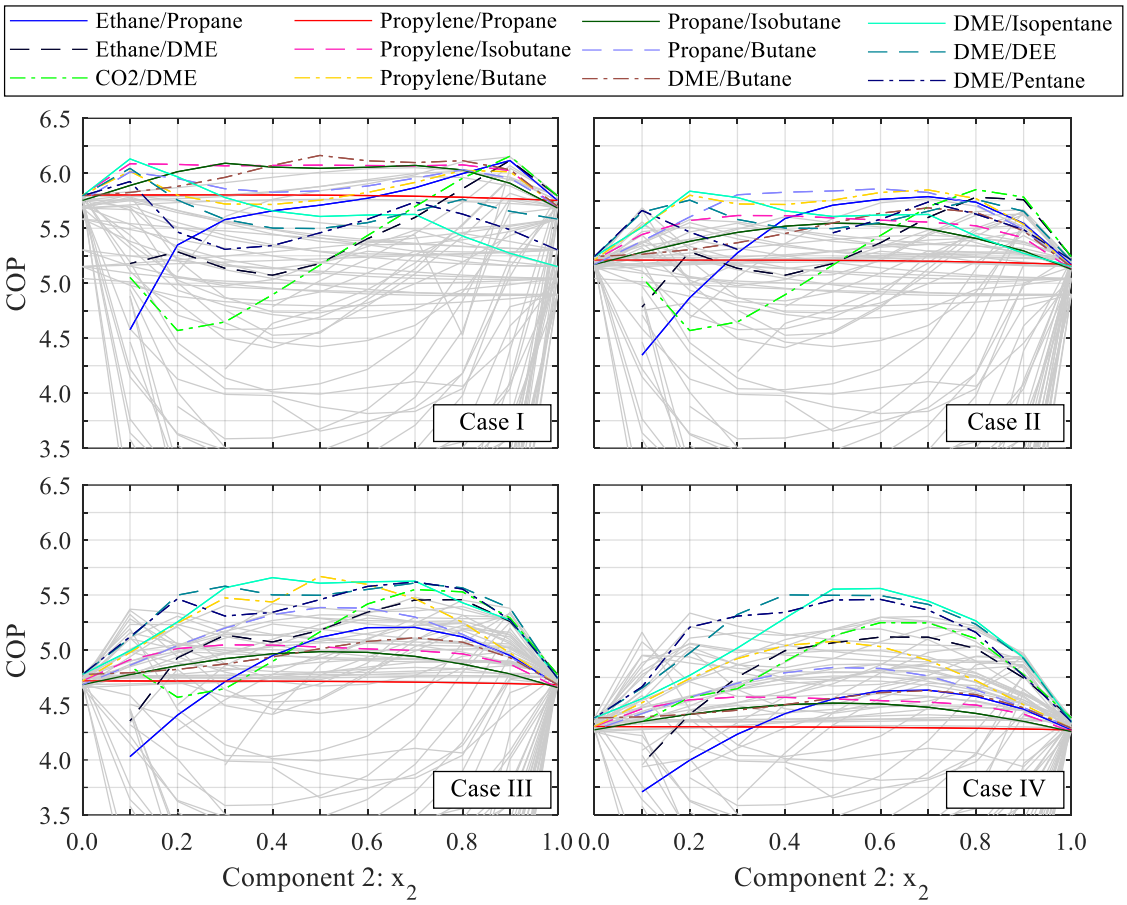

Figure 4: COP for all cases with minimum 0 K superheating for all simulations over the composition of the less volatile component 2. Selected mixtures are labelled while other mixtures are included as grey shaded, representing the general solution space.

Figure 5 indicates a similar trend of fluids with a good performance, defined by having an exergetic efficiency higher than 0.45, for all four cases. The solutions with a good performance are typical accumulated with low values of the glide match indicators in the source and higher indicator values showing a moderate mismatch in the sink around 3 for case I and between 2 and 3 for case IV. There were also solutions with an almost optimal glide match in the sink (indicator values lower than 2) and an increased mismatch in the source (indicator values around 4 in case I and around 3 in case IV) which have a moderate performance. Nevertheless, only few solutions could be found in the range of an optimal glide match with indicator values for both sink and source of less than 2.2 for case I to 1.5 for case IV. Especially for the cases with low indicator values for both the source and sink glides, these solutions were mostly transcritical solutions with a good match on the sink side and a more moderate glide match on the source side.

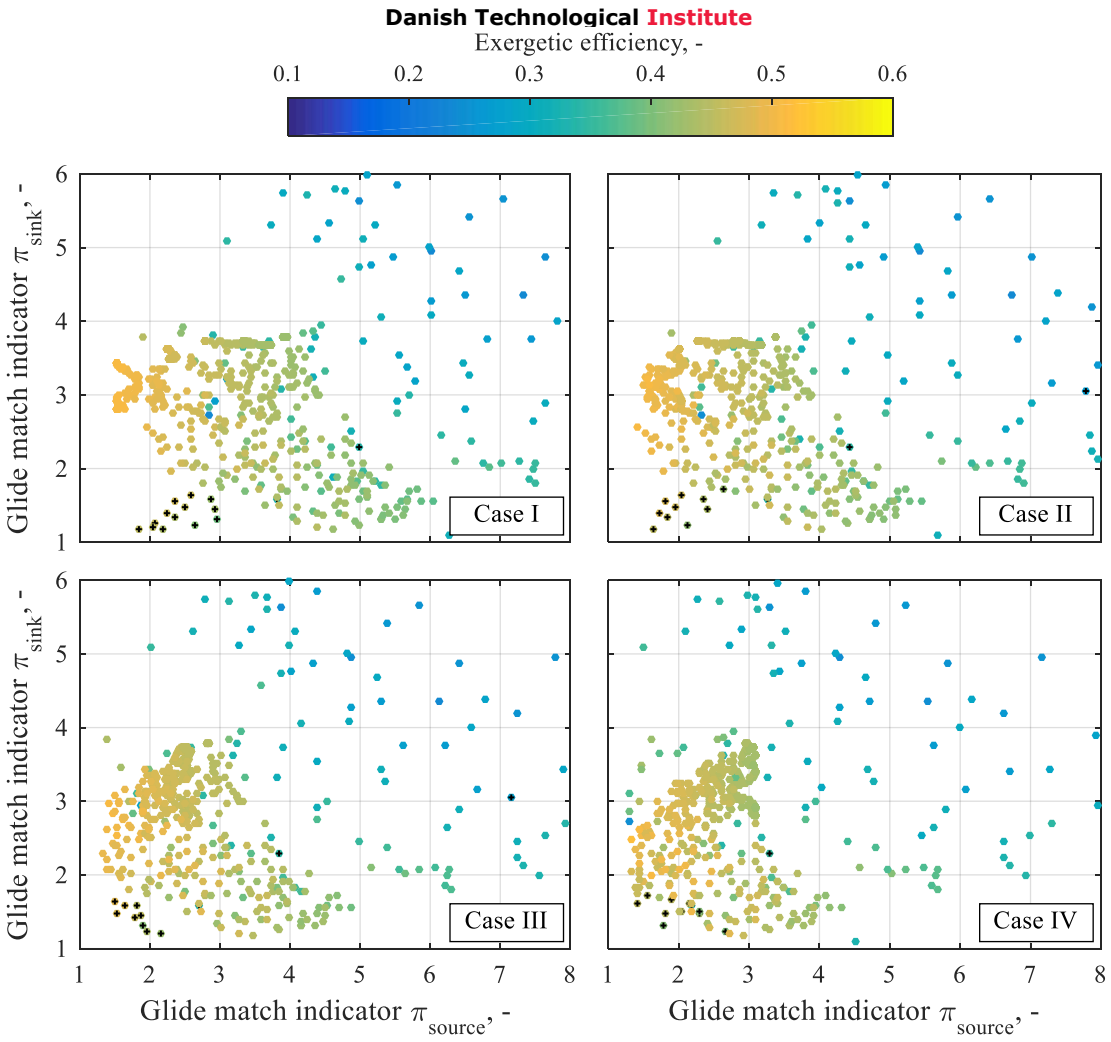

Figure 5: Combinations of glide match indicators π of sink and source for all simulations for case I-IV with 5 K superheat with exergetic efficiency indicated by colour, transcritical cycles are marked with a black +.

The diagrams in Figure 5 show that a large range of possible temperature profiles is covered, while the dependency between the source glide match and exergetic efficiency shows a clearer pattern than for the sink. This dependency can be seen more clearly in Figure 6, in which the glide match indicator of the source (left) and of the sink (right) are plotted over the exergetic efficiency for all cases superimposed on each other. The source glide match indicator varies between 1 and 15, while the exergetic efficiency can be low irrespective of a good glide match. Nevertheless, an increasing exergetic efficiency requires an enhanced temperature glide match. Thus, to obtain a good performance a good glide match in the source can be seen as a requirement.

The diagram on the right-hand side of Figure 6 shows a different pattern for temperature glide match in the sink over the exergetic efficiency. An increasing mismatch results in a decreased performance as well, whereas here a matching indicator below 4 enables exergetic efficiencies from 0.25 to 0.55. In this region the efficiency is dominated by the source side, which is indicated by the colour. While optimal glide matches in the sink result in an exergetic efficiency between 0.4 and 0.5, the highest exergetic efficiencies are obtained with a glide match indicator value in the sink of approximately 3.

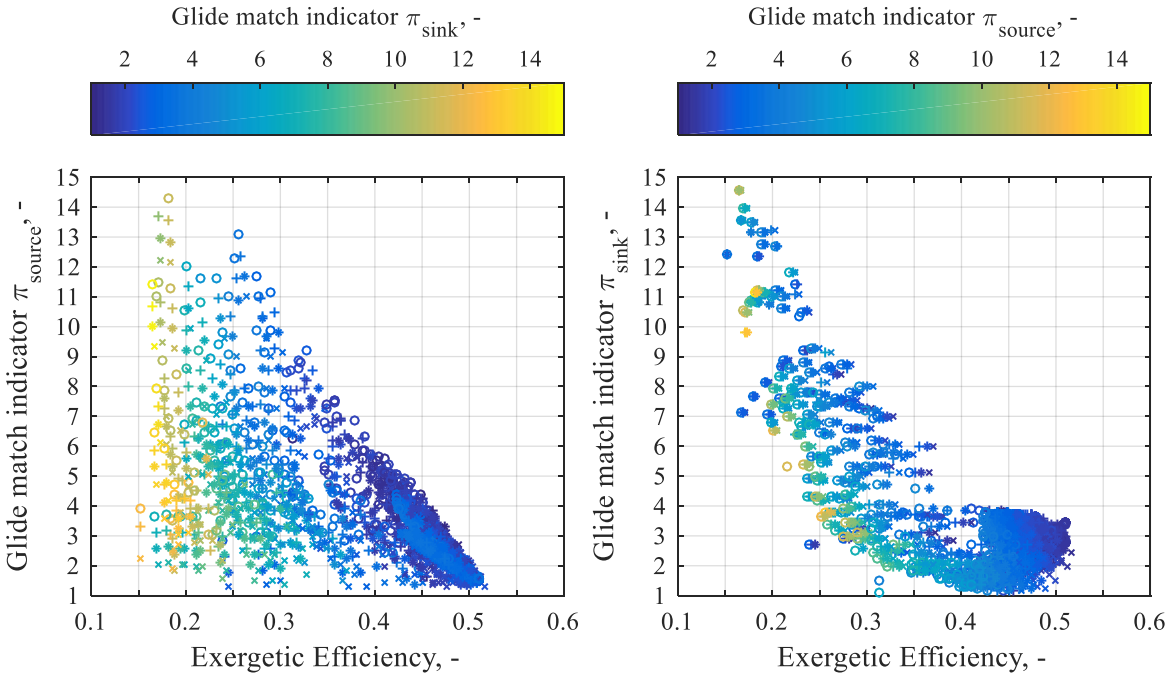

*Figure 6: Glide match indicators for source (left) and sink (right) over exergetic efficiency with indication of respective other heat transfer process by colour for all cases indicated by marker (Case I: o, Case II: +, Case III: *, Case IV: x).*

The diagrams in Figure 7 to Figure 10 show temperature – heat load diagrams for relevant and characteristic cases. Figure 7 shows the mixture 10 % Ethane – 90 % Propane for case II which represents one of the best solutions in terms of COP and represents a good compromise between glide matches on both sides. The 80 % Ethane – 20 % Propylene mixture shows an almost perfect glide match in sink and source, but a decreased COP compared to the best pure fluids for case II.

Figure 9 and Figure 10 show cases in which either the source or sink had a good glide match while the other glide match was moderate without significantly reducing the COP. The exergy destruction caused by the mismatch of the fluid in source and sink for the case shown Figure 9 are $y^*_{D,fluid,source}$ = 5.5 % and $y^*_{D,fluid,sink}$ = 25 %, whereas for the case of Figure 10 they contribute with $y^*_{D,fluid,source}$ = 26 % and $y^*_{D,fluid,sink}$ = 2.5 %.

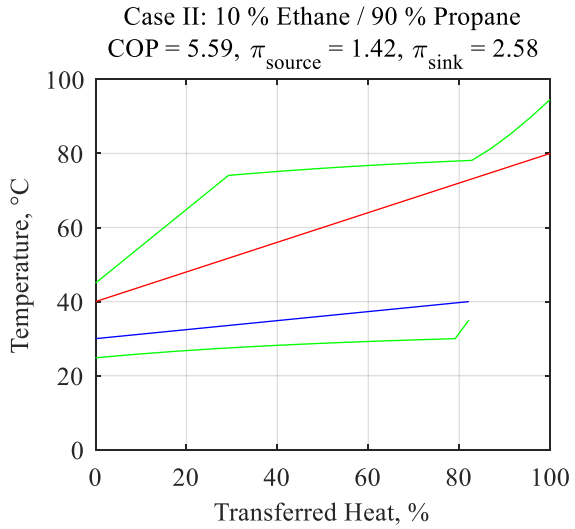

Figure 7: Temperature-Heat-Diagram for subcritical cycle with a good glide match on the source side, a moderate glide match on the sink side and a good COP.

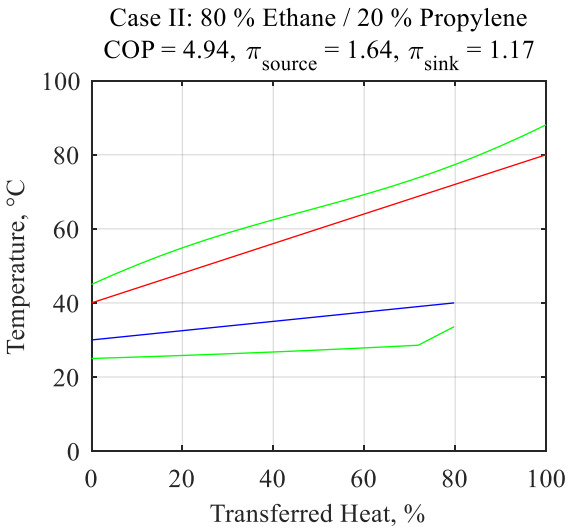

Figure 8: Temperature-Heat-Diagram for a transcritical cycle with a good glide match on both the source and sink side and a moderate COP.

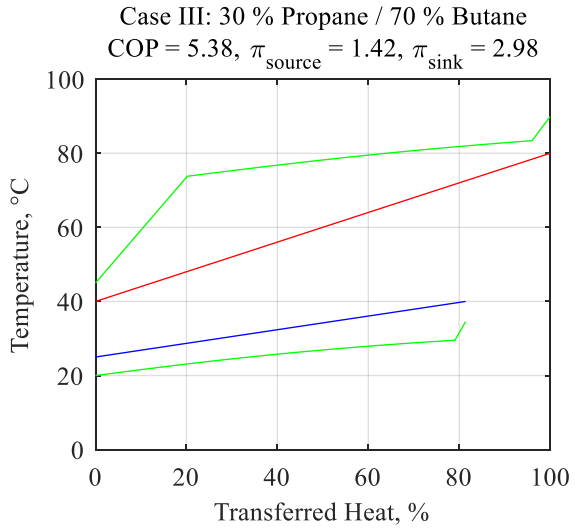

Figure 9: Temperature-Heat-Diagram for a subcritical cycle with a good glide match on the source side, a moderate glide match on the sink side and a good COP.

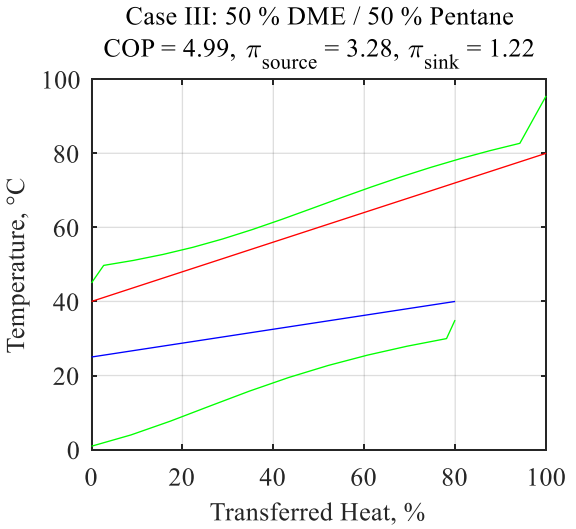

Figure 10: Temperature-Heat-Diagram for a subcritical cycle with a poor glide match on the source side, good glide match on the sink side and a moderate COP.

3.2.4. Discussion

The presented work has analysed the potential performance increase which can be achieved from a suitable choice of a working fluid mixture. The choice of the working fluid and thus, also the possible performance increase is strongly dependent on the cycle layout. The shown case assumed a required minimum superheating of 5 K, which required a smaller temperature glide in the evaporator and thereby decreased the improvement potential of zeotropic mixtures. The simulations of the cases without superheating showed an increased potential for zeotropic mixtures, whereas case I without the minimum 5 K superheating and 5 K temperature glide shows similar results as case II with no superheating and 10 K temperature glide. The feasibility of reducing the required minimum superheating depends on the equipment and can be enabled by different approaches. Another measure to enable operation without superheating within the evaporator is the utilization of an internal heat exchanger.

The miscibility of the considered mixtures was analysed and binary mixtures with DME were identified to be potentially immiscible, which would result in a system with two liquid phases of different compositions. Since the results have shown that DME performs well in many mixtures, the miscibility of the specific composition at the required pressures and temperatures was analysed. The miscibility gaps occurred in all cases below operation temperatures, which yields a full miscibility of the components in the required range of pressure and temperature.

Different variables were analysed with respect to their usability and meaningfulness for evaluations of different working fluid mixtures and comparisons with other solutions. The introduced temperature glide matching indicator accounts for the exergy destruction due to the fluid being non-ideal as a dimensionless, linear indicator. The exergy destruction of the fluid is put into relation to the heat transfer process and therefore can be used to compare processes with different loads in heat sink and source and among different simulations with varying overall efficiencies. If the exergy destruction is e.g. put into relation to a value which depends on the cycle performance, such as the exergetic fuel or overall exergy destruction, the results from different simulations cannot be compared to each other. The temperature glide match indicator represents a quantitative measure of the glide match and has proven to give meaningful results.

The results suggest a stronger dependency of the cycle performance on the glide match in the source than in the sink. This dependency is supported by the structure of equation 3 in which the absolute temperatures of the heat transfer process contribute squared in the denominator to the exergy destruction from heat transfer over a certain temperature difference. Assuming the heat to be transferred at the thermodynamic average temperature of sink stream (332.7 K) and source stream (310.6 K) the exergy destruction per unit transferred heat in the source is approximately 15 % higher than in the sink. An increasing mismatch will furthermore intensify this effect, since the temperature differences and thus the absolute temperatures diverge. Nevertheless, the higher heat load in the sink compensates this effect to some extent.

Different cases have been shown representing the different available combinations of temperature glides and accordingly different qualities in glide matching. Often a good compromise between both has shown to give good COPs. Nevertheless, Figure 8 has shown

a case with an optimal glide match and a COP which is not as optimal as the glide match suggests. Since the compressor and the throttling valve were modelled with the same efficiency it can be concluded that there are fluid properties influencing the exergy destruction in the remaining components to a relevant extent.

The cases presented in Figure 9 and Figure 10 show some inefficiencies due to heat transfer but based on the high COPs it can be assumed that the working fluids do not have an unfavourable effect on compressor and throttling valve. If in these cases the temperature glide match could be improved by any cycle adjustment while retaining the fluid and the remaining components constant, the exergy destruction in the component and thus, in the entire system would decrease and improve the performance. Possible cycle adjustments are extensively discussed for water ammonia systems. The theoretical potential of decrease in exergy destruction is around 25 % for the presented cases.

The variety of the results demonstrated the various possibilities, in which the medium properties influence the performance of the different components and accordingly the overall performance of the system. These manifold interdependencies imply the difficulty to provide recommendations for selecting mixture components dependent on the boundary conditions.

3.3. Subtask 2: Evaluation of Advanced Cycle Configuration

As the results of subtask 1 indicates then, although the use of zeotropic mixtures can significantly increase the performance of heat pumps, then the optimal solutions using a simple one-stage cycle still infers a significant mismatch of temperature glide mainly in the condenser. This mismatch subsequently entails heat transfer irreversibilities, which again leads to a reduction of the COP. Hence, further improvements could be found if a better glide match could be attained. As shown from the results of subtask 1 a better match cannot be attained only by selecting the best fluid and hence requires a more advanced cycle layout.

Further, the results of subtask 1 also indicate that avoiding superheat in the evaporator entails a significant COP improvement when utilizing zeotropic mixtures. The objective of subtask 2 is thus to identify suitable advanced cycles that can ensure both stable operations, without evaporator superheat, and increased glide matching possibilities.

3.3.1. Methods

3.3.1.1. Identification of Advanced Cycle Configurations

A total of eight cycle configurations have been modelled and simulated in the present analysis. As the base case the simple one-stage heat pump configuration was included, as seen in Figure 11a. As seen, this is a standard one stage heat pump comprised of a compressor, condenser, expansion valve and evaporator. In the present analysis the cycle was assumed to operate with a superheat of 5 K at the outlet of the evaporator.

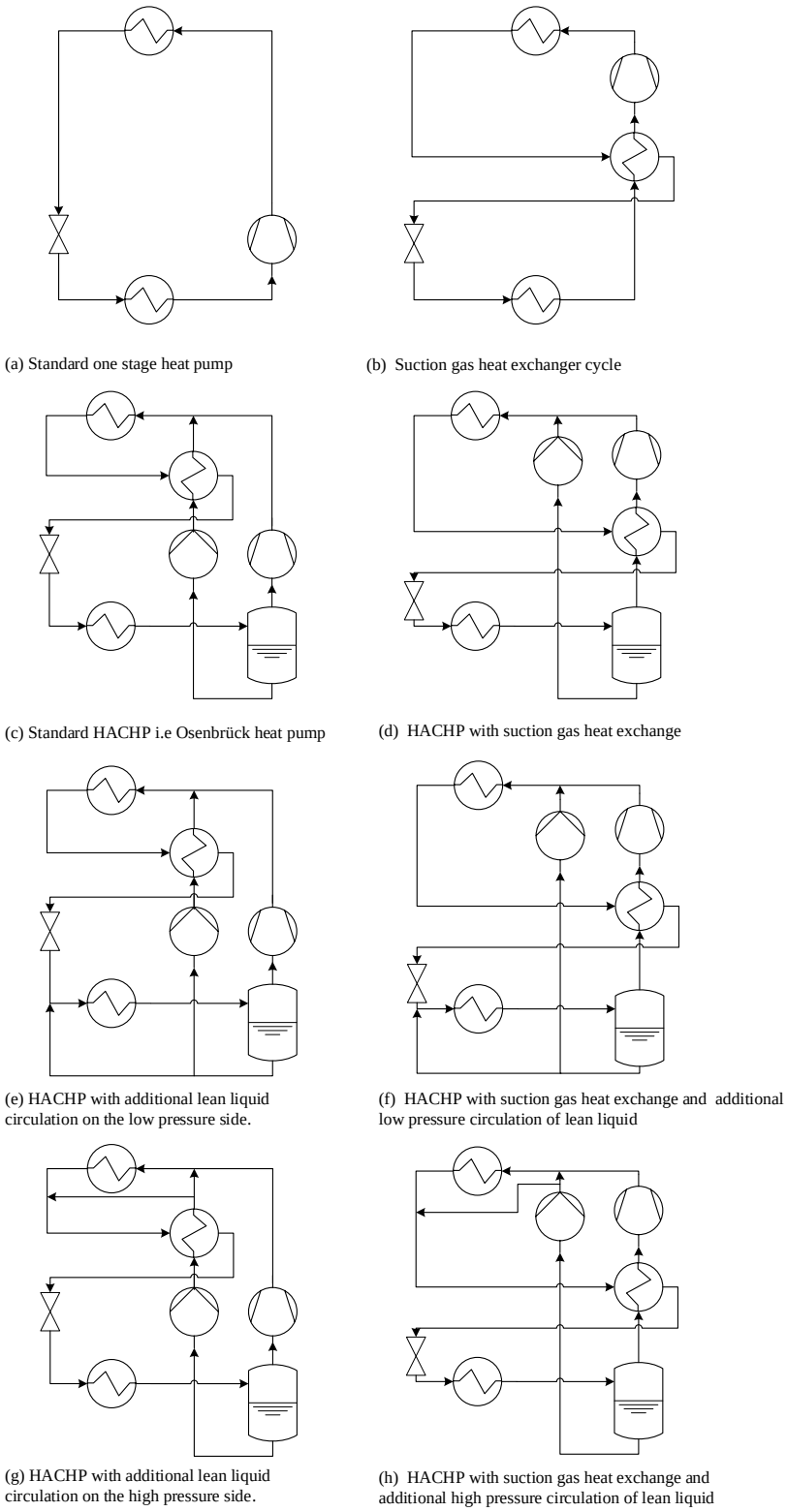

(a) Standard one stage heat pump

(b) Suction gas heat exchanger cycle

(c) Standard HACHP i.e Osenbrück heat pump

(d) HACHP with suction gas heat exchange

(e) HACHP with additional lean liquid circulation on the low pressure side.

(f) HACHP with suction gas heat exchange and additional low pressure circulation of lean liquid

(g) HACHP with additional lean liquid circulation on the high pressure side.

(h) HACHP with suction gas heat exchange and additional high pressure circulation of lean liquid

Figure 11. Investigated cycle configurations. Standard one stage cycle (STD) and an internal exchanger cycle in which the suction gas is heated before the compression (SGHEX). HACHP with three different circulation options for the lean liquid: standard, additional low pressure circulation and additional high pressure circulation. Further, two different internal heat exchanger placements: heating the high pressure lean liquid or heating the suction gas. Combining the three different circulation options and two heat exchanger configurations totals the six different HACHP configurations seen.

Further, a suction gas heat exchanger cycle was included in the analysis. This is shown in Figure 11b. As seen this configuration is similar to the standard cycle but with an internal heat exchanger placed between the liquid line prior to the expansion valve and the suction line prior the compressor. The suction gas cycle was assumed to operate with saturated conditions at the outlet of the evaporator, hence all superheat was attained in the internal heat exchanger.

Apart from the two configurations of the standard heat pump, a number of different configurations of the hybrid absorption-compression heat pumps (HACHP) was included in the analysis. These may be seen in Figure 11c-h. Figure 11c shows the standard HACHP configuration. As seen here the outlet of the evaporator is a two-phase mixture and thus a liquid vapour separator was imposed to separate the two phases. The saturated vapour extracted from the top of the tank is supplied to the compressor while the saturated liquid extracted from the bottom of the tank is supplied to the liquid pump.

A HACHP in which the internal heat exchanger was placed in the suction gas line, as seen in Figure 11d, has also been modelled and simulated. As seen the only difference to the standard HACHP was the internal heat exchanger placement.

Both HACHP seen in Figure 11c & d have one additional degree of freedom compared to the standard heat pump seen in Figure 11a. In this analysis the additional degree of freedom has been satisfied by setting the circulation factor, f_1. The circulation factor, f_1, was defined as the ratio between the lean liquid extracted from the liquid vapour separator, $\dot{m}_{l,}$, and the total mass flow supplied to the separator, $\dot{m}_r$. It is thus directly linked to the vapour quality, $q_{\text{evap,out}}$, at the outlet of the evaporator.

$$f_1 = \frac{\dot{m}_l}{\dot{m}_r} = \frac{\dot{m}_l}{\dot{m}_v + \dot{m}_l} = 1 - q_{\text{evap,out}}$$

Further, two additional internal liquid circulation lines have been analysed. The first option was an additional circulation on the low-pressure side. These may be seen in Figure 11e & f with the lean liquid and suction gas heat exchanger, respectively. As seen the additional low-pressure circulation was achieved by taking a part of the saturated lean liquid extracted from the liquid vapour separator and mixing it with the stream entering the evaporator.

This again supplies one additional degree of freedom, which was satisfied by defining an additional circulation factor, f_2. This was defined as the ratio of the mass flow of lean liquid circulated at the low pressure, $\dot{m}_{l,\text{LP}}$, relative to the total mass flow of lean liquid, $\dot{m}_l$. Hence, if $f_2 = 0$ then no mass flow was circulated at the low pressure and the cycle effectively returns to the layouts seen in Figure 11c & d. Conversely, if $f_2 = 1$ then all the lean liquid extracted from the liquid vapour separator was circulated at the low pressure and thus no mass flow was supplied to the liquid pump.

$$f_2 = \frac{\dot{m}_{l,\text{LP}}}{\dot{m}_l}$$

Finally, an additional high-pressure circulation option was included as seen in Figure 11g & h, again with the lean liquid and suction gas heat exchanger, respectively. As seen the high pressure circulation was achieved by taking a part of the lean liquid and bypassing it from the condenser. Again, an additional circulation factor, f_3, was defined to satisfy the

additional degree of freedom. Similarly, this was defined as the ratio of the mass flow of lean liquid, which is bypassed from the condenser, $\dot{m}_{l,\mathrm{HP}}$, relative to the total mass flow of lean liquid supplied to the high pressure side. Hence, if $f_3 = 0$ then no mass flow was circulated at the high pressure and the cycle effectively returns to the layouts seen in Figure 11c & d. Conversely, if $f_3 = 1$ all the lean liquid bypasses the condenser.

$$f_3 = \frac{\dot{m}_{l,\mathrm{HP}}}{\dot{m}_l - \dot{m}_{l,\mathrm{LP}}}$$

The hypothesis for increasing the heat pump performance by applying different variations of internal liquid circulation is that the liquid circulation allows control of the temperature glide experienced in the evaporator and condenser. This is sketched for the standard HACHP in the Temperature-Enthalpy diagram seen in Figure 12. As seen, when the liquid circulation rate is increased the outlet of the evaporator and the inlet of the condenser moves towards the saturated liquid line, effectively decreasing the temperature glide in the condenser and evaporator. The HACHP concept is thus beneficial for mixtures where the saturation temperature difference (temperature difference between saturated liquid and vapour at the same pressure) is greater than the temperature difference of the sink and source. In these cases, the HACHP concept can be used to increase the glide match and thus possibly increase the efficiency. The penalty for the increased glide match is the irreversibility related to the mixing of the hot compressor discharge gas and the cooler pumped liquid. In some cases, this negative contribution may exceed the benefit attained by the glide match and thus the heat pump will not experience a net performance increase.

Further, as may be seen in both Figure 12 and Figure 13, for the HACHP the temperature difference in the condenser and evaporator will be in same range regardless for the liquid circulation rate. Hence, this configuration is mainly beneficial if the sink and source glides are in the same range. In case one of these are significantly greater than the other, glide match cannot be attained simultaneously in both the condenser and evaporator. In these cases, the additional low-pressure or high-pressure liquid circulation may allow a better glide match and thus may further increase the performance. This is attained as the addition of either low or high pressure liquid circulation will result in a different working fluid composition in the evaporator and condenser. As seen in Figure 13 the composition of the working fluid also as a significant effect on both the curvature and magnitude of the temperature glide. Hence, by combining the standard HACHP with either the low-pressure or high-pressure liquid circulation the additional degree of freedom can be used to attain a better glide match. However, a penalty must again be expected related to the mixing of streams with different temperatures and compositions.

None of the three circulation factors can generally be chosen as fixed values but will have to be optimized for the specific fluid and operating condition in order to attain the best COP. An optimization of the circulation factor has thus been applied for all simulated fluids, compositions and operating conditions.

To ensure controllable and reliable operation of the system the value of f_1 was limited to values >0.05, as letting $f_1 = 0$ would result in a standard one stage cycle with no superheat which is not regarded as technically feasible solution. The circulation factors f_2 and f_3 have been optimized in the full range of meaningful values, i.e. 0-1.

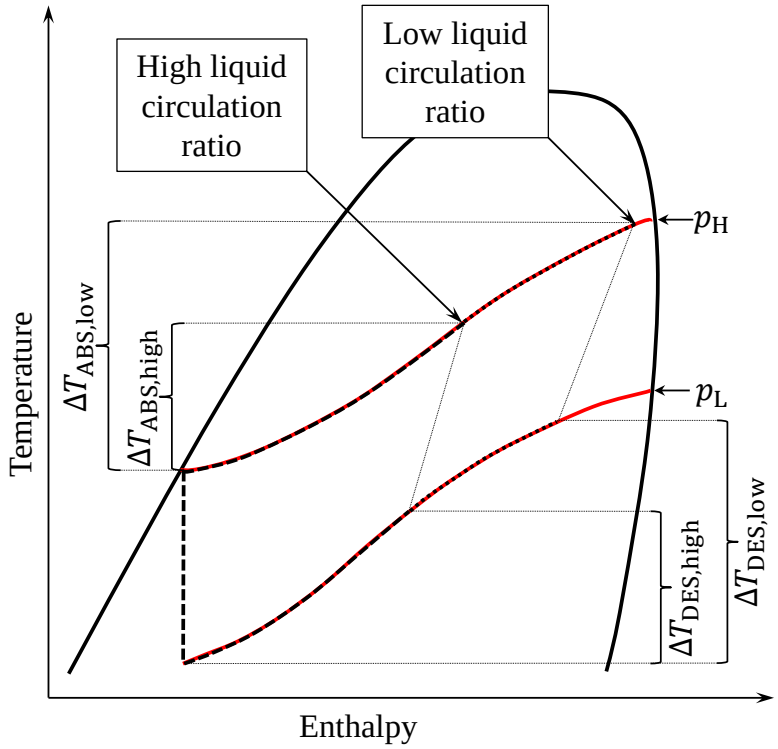

Figure 12. Sketch of the influence of liquid circulation ratio on the temperature glide during phase change in the evaporator and condenser.

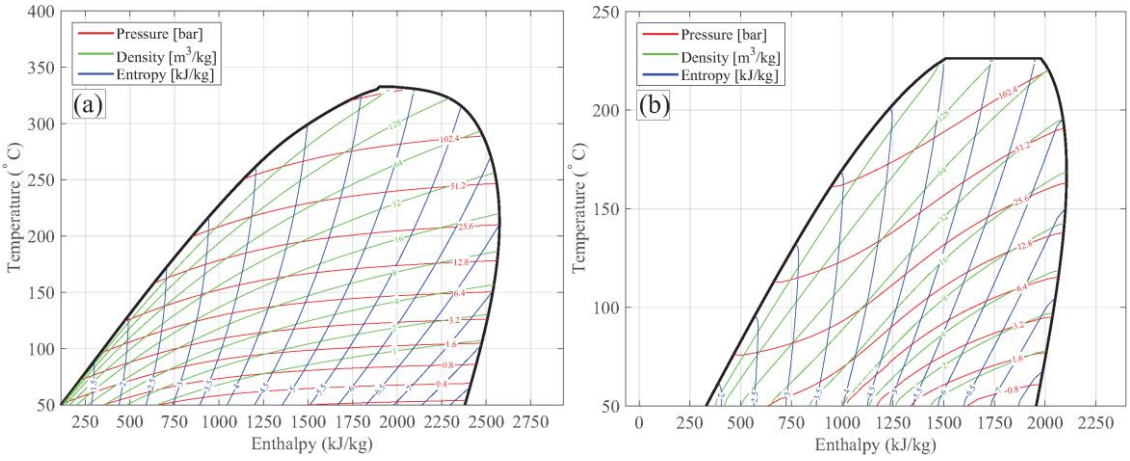

Figure 13. Temperature – Enthalpy diagrams for ammonia-water mixtures with ammonia concentrations of 25 % (a) and 75 % (b).

3.3.1.2. Modelling of Advanced Cycle Heat Pump

The models for the advanced cycles was developed using the same framework as used to model the simple cycles in subtask 1 and thus is again based on the First and Second Law of Thermodynamics and includes energy and mass balances for all components. Trans-critical operation was not considered for the HACHP concepts.

In order to calculate condensation and evaporation pressures a minimum pinch point temperature difference of $\Delta T_{\mathrm{pinch,min}} = 5\ \mathrm{K}$ was introduced. This value was equally applied to the internal heat exchangers. The possible performance gain from subcooling is always completely exploited by defining the subcooler outlet temperature by the pinch point temperature difference above the sink inlet temperature.

The compression process was modelled with an isentropic efficiency of $\eta_{\mathrm{comp,is}} = 0.8$ while losses from the electrical motor to the environment were disregarded. The volumetric heating capacity VHC relates the supplied heat load to the volume flow rate at the inlet of the compressor and indicates the size of the component.

The throttling process was assumed to be isenthalpic.

The model was implemented in Matlab and used medium properties from Refprop 10 with the recommended state of the art models for the equations of state and mixing parameters for all modelled fluid mixtures.

3.3.1.3. Refrigerant Screening

In order to determine when the different cycle configurations are advantageous a total of eight different operating conditions have been analysed. These are seen in Table 4. The general approach has been to combine high and low values of sink and source temperature difference with high and low temperature lifts.

Table 4: Definition of boundary conditions for considered cases.

Case Number	Heat Source $T_{\mathrm{source,in}} \rightarrow T_{\mathrm{source,out}}$	Heat Sink $T_{\mathrm{sink,in}} \rightarrow T_{\mathrm{sink,out}}$
I	40 °C → 35 °C	45 °C → 50 °C
II	40 °C → 10 °C	45 °C → 50 °C
III	40 °C → 35 °C	45 °C → 75 °C
IV	40 °C → 10 °C	45 °C → 75 °C
V	40 °C → 35 °C	65 °C → 70 °C
VI	40 °C → 10 °C	65 °C → 70 °C
VII	40 °C → 35 °C	65 °C → 95 °C
VIII	40 °C → 10 °C	65 °C → 95 °C

A total of 21 fluids were included in the analysis, these may be seen in Table 5, these include both natural refrigerants i.e. hydro-carbons, ammonia, CO_2 and water, HFOs and a single HFC. The first 19 fluids have all been mixed in every combination while ammonia and water (20 and 21) have only been mixed with each other. All mixtures were simulated in composition ranges from 0.1 to 0.9 with 0.1 increments.

Table 5: List of fluids considered in the design of binary mixtures above dashed line and additionally considered fluids below dashed line.

No	Name of Fluid	Ref. No.:	Type	ODP -	GWP -	Normal Boiling Point. °C	Crit. Temp. °C	Crit. Pres. bar	Safety Class
1	Methane	R50	HC	0	25	-161.5	-82.6	46.0	A3
2	Ethylene	R1250	HO	0	6.8	-103.8	9.2	50.4	A3
3	Ethane	R170	HC	0	2.9	-88.6	32.2	48.7	A3
4	CO_2	R744	Nat.	0	1.0	-	31.0	73.8	A1
5	Propylene	R1270	HO	0	3.1	-47.6	91.1	46.7	A3
6	Propane	R290	HC	0	3.0	-42.0	96.7	42.5	A3
7	Dimethylether (DME)	RE170	HC	0	1.0	-24.0	127.3	53.4	A3
8	Iso-Butane	R600a	HC	0	3.0	-11.7	134.7	36.3	A3
9	n-Butane	R600	HC	0	3.0	-0.5	152.0	38.0	A3
10	Iso-Pentane	R601a	HC	0	4.0	27.8	187.3	33.8	A3
11	Ethylether (DEE)	R610	HC	0	4.0	34.6	193.7	36.4	A3
12	Pentane	R601	HC	0	4.0	36.1	196.6	33.7	A3
13	n-Hexane		HC	-	-	68.7	234.5	30.3	-
14	Heptane		HC	-	-	98.4	267.0	27.4	-
15		R1234yf	HFO	0	4.0	243.6	367.8	33.8	A2L
16		R1234ze(E)	HFO	0	7.0	254.1	382.5	36.3	A2L
17		R1234ze(Z)	HFO	0	10	282.8	423.2	35.3	-
18		R1233zd(E)	HFO	0	4.5	291.4	439.6	36.2	A1
19		R134a	HFC	0	-	247.0	374.2	40.5	A1
20	Ammonia	R-717	Nat.	0	0.0	-33.3	132.4	112.8	B2
21	Water	R-718	Nat.	0	0.2	100.0	373.9	220.6	A1

3.3.2. Results

3.3.2.1. Standard and Suction Gas Heat Exchanger Cycle

Figure 14 shows the COP as a function of the mixture composition for the mixtures pentane-heptane and isobutene-DEE both under operating condition case IV. As seen both the standard one stage heat pump (STD) and suction gas heat exchanger (SGHEX) cycles are capable of increasing the COP compared to the best pure components. Further, it is seen the SGHEX is better than the STD at all compositions and that the performance increase seems to be higher for the mixtures than for the pure components. SHGEX can thus attain a significant increase in COP compared to the STD and even attains a higher COP increase at compositions at which the STD cycle operates with a high performance.

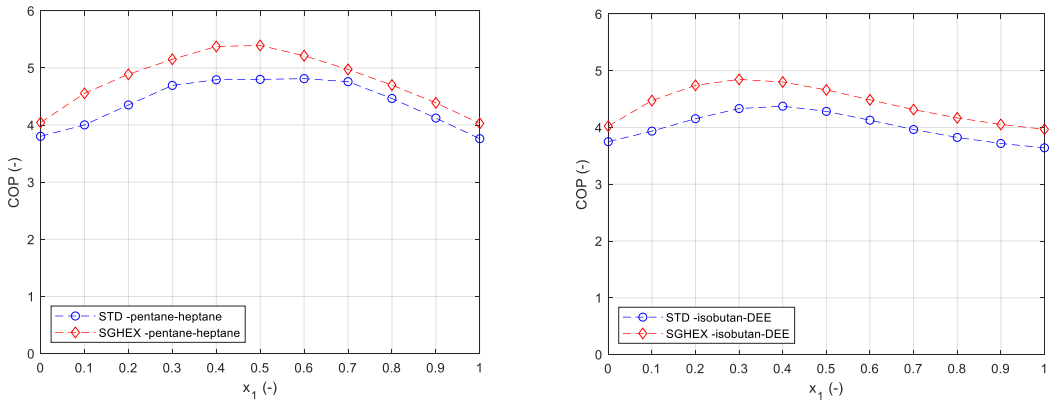

Figure 14. Comparison of the STD and SGHEX cycle for the mixtures pentane-heptane and isobutene-DEE. Both for operating condition case IV.

3.3.2.2. HACHP

In order to get a grasp of how the different mixtures will react to the different liquid circulation options, results for selected mixtures will be presented. These results will present the relation between the heat pump performance and the liquid circulation ratios. These results will show that all the cycles presented in Figure 11 have the ability to further increase the performance.

3.3.2.3. Standard HACHP

Figure 15 shows how the COP changes when the liquid circulation factor is changed. As seen, this is presented for the mixtures pentane-heptane and ammonia-water. Further, this is presented for a range of compositions for both mixtures. As seen the two mixtures react very differently to the application of liquid circulation. The pentane-heptane mixtures experience a decrease in COP for all the presented composition and thus for this mixture the circulation rate should be set as low as technically feasible. Conversely, the ammonia-water mixture experiences a significant increase in COP from the application of liquid circulation showing a well-defined optimum circulation rate for all presented compositions. Further, from the results for the ammonia-water mixture it is clear that the optimum circulation rate depends also on the composition of the mixture. In this case the higher the ammonia concentration the lower the optimum circulation rate is.

The results presented in Figure 15 emphasises the need to identify suitable circulation rates for each individual mixture, composition and operating condition. Further, the results show that while some mixtures, such as ammonia-water rely on the application of liquid circulation to attain a competitive performance other such as a pentane-heptane mixture suffers a performance decrease due to the application of the liquid circulation.

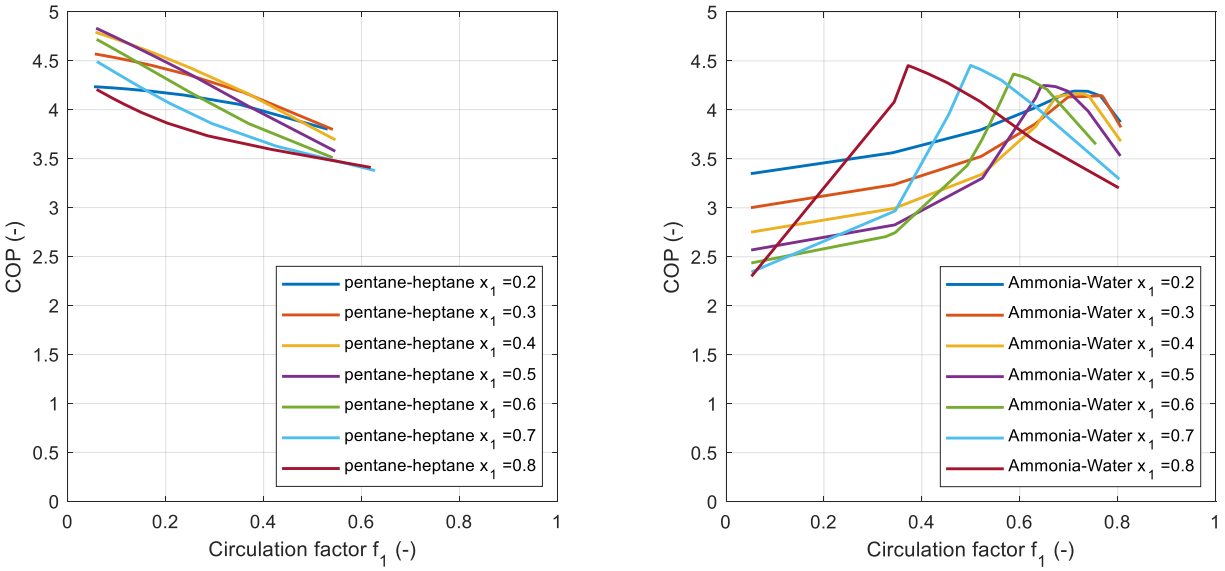

Figure 15. COP as a function of liquid circulation factor f_1 over a range of compositions for the mixtures pentane-heptane (left) and ammonia-water (right). Both are presented for Case IV with a standard HACHP.

3.3.2.4. Low Pressure Liquid Circulation

Figure 16 exemplifies the application of the additional low-pressure liquid circulation. This is presented for two mixtures: 70 % pentane-heptane under operating conditions case V, and 80 % DEE-heptane under operating condition case III. Again, two different trends are observed for the two mixtures. For the pentane-heptane mixture the optimum COP is located at f_1=0.48 and f_2=0.4 and thus this mixture benefits from having both the conventional HACHP liquid circulation but also the additional low-pressure liquid circulation. For the DEE-heptane mixture the optimum COP is located at f_1=0.31 and f_2=0.0 and thus to optimise this mixture none of the liquid extracted from the liquid vapour separator should be supplied to the high pressure pump but rather completely supplied to the low-pressure liquid circulation line.

Further, mixtures that do not benefit from low-pressure circulation have also been observed again highlighting the need to select suitable circulation rates.

3.3.2.5. High Pressure Liquid Circulation

Figure 17 exemplifies the use of the high pressure liquid circulation option. Here for the two mixtures 70 % DEE-heptane and 60 % Hexane-Heptane, both for case V. As seen the performance of the mixture DEE-heptane can be increased by the application of high pressure liquid circulation while the mixture DEE-heptane does not benefit from this.

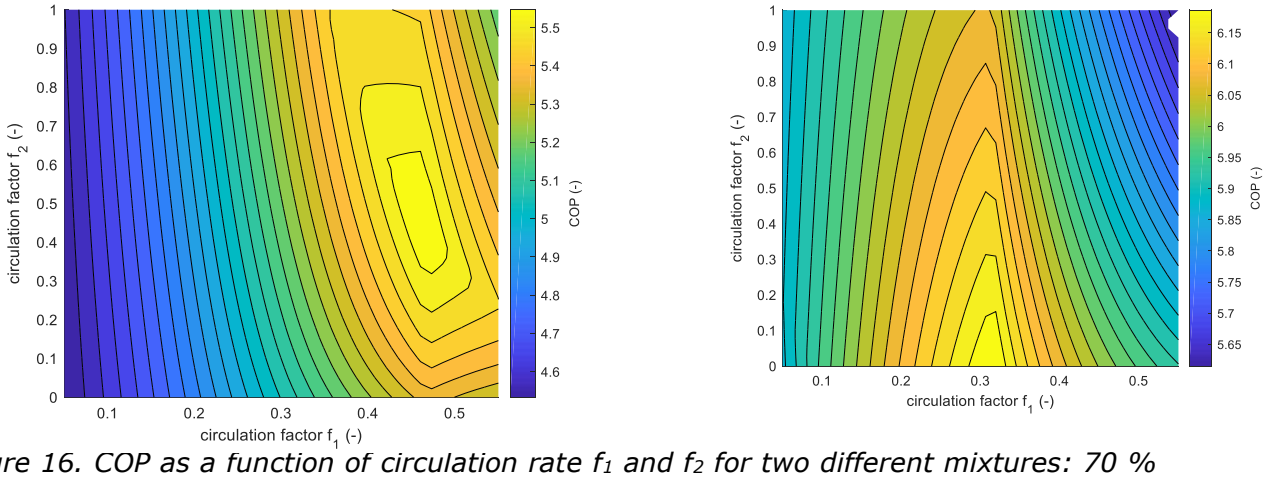

Figure 16. COP as a function of circulation rate f_1 and f_2 for two different mixtures: 70 % pentane-heptane for case V (left) and 80 % DEE-Heptane for case III (right), both with low pressure liquid circulation.

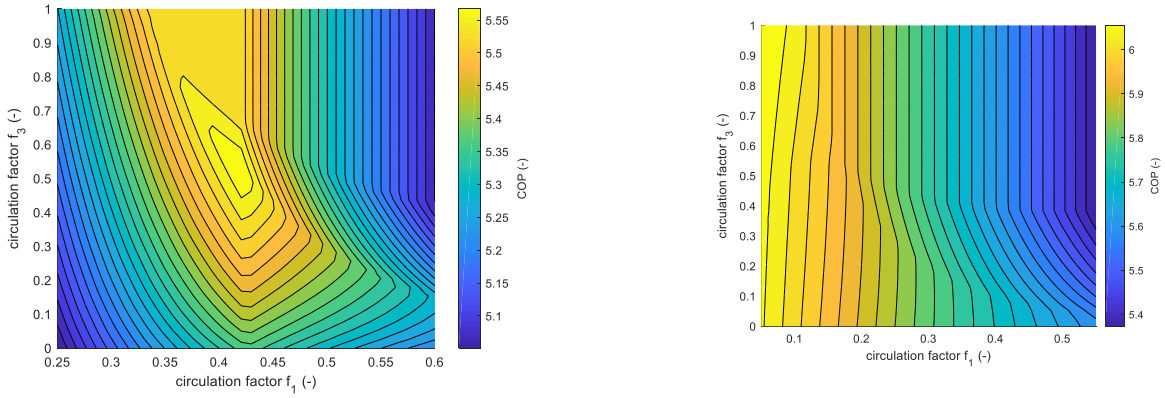

Figure 17. COP as a function of circulation rate f_1 and f_3 for two different mixtures: 70 % DEE-Heptane (left) and 60 % Hexane-Heptane (right). Both for case V with high pressure liquid circulation.

3.3.2.6. Refrigerant Screening

As shown in the previous section all the analysed advanced cycles are capable of increasing the performance for specific mixtures under specific operating conditions. However, to which extent these improvements can result in more efficient heat pumps when the designer can freely choose fluids and compositions is still unclear. To investigate this, all the suggested cycles have been simulated with all the possible combinations of the refrigerants presented. This is further done for all eight operating condition cases.

The results of the screening are presented first in Figure 18. Here the results for all the HACHP are presented by their COP and the optimum liquid circulation rate f_1. Further, the best COP of all the suggested cycles are presented by the vertical lines. Further, the colour of the markers indicates the saturation temperature difference of the utilized mixture.

A number of relevant results can be extracted from Figure 18. First of all, a large concentration of solutions can be observed at the minimum circulation rate of 0.05. This is the same for all eight cases. These are all the mixtures that do not benefit from liquid circulation. It can be seen that these mixtures yield COPs in the full range of possible

solutions and further that the mixtures also have the full range of saturation temperature differences. Hence, not all mixtures for which the saturation temperature difference is greater than that of the sink and source will benefit from liquid circulation. Secondly, it is seen that a larger number of mixtures benefit from liquid circulation and that the overall trend for these solutions is that the larger the saturation temperature difference the larger the circulation rate should be. However, this also reveals the trend that the higher the needed circulation rate is the lower the COP will be. This as when the need for increased liquid circulation rate goes up, in order to match the glide, then the mixing irreversibilities also goes up thus reducing the COP.

Further, it may be seen that the highest COP for all eight cases is attained by the SGHEX cycle, however for most of the eight operating condition this is followed closely be several of the HACHP cycles.

Table 6 summarizes the COP of the best fluid for all 8 cycles under all 8 operating condition cases. The results for the STD and SGHEX cycle are further presented for both the best pure fluid and the best mixture. Pure fluids have not been evaluated in the HACHP cycles as these cycle layouts are not a sensible solution for pure fluids.

The results of Table 6 thus summarize the results of the complete refrigerant screening. It can be seen that, as mentioned earlier, the best performance is always attained by the SGHEX cycle. However, for some of the cases different variation of the HACHP offers a comparable performance. For all the optimum fluids the best performance was attained with the internal heat exchanger placed in the suction gas rather that the lean liquid. This is most likely related to the fact that apart for the HACHPs in cases 1 and 4 all HACHPs have the optimum performance at $f_1 = f_{min} = 0.05$. In this case only a very small mass flow will be supplied to the liquid pump and therefore the low capacity rate of the cold stream in the internal heat exchanger will result in a low heat load. Hence, more internal heat recovery is attained with the suction gas heat exchanger placement. The fact that most of the optimum cycles run with the minimum liquid circulation rate further indicates that the selection of the appropriate fluid is dominant over selection of the appropriate cycle.

Further, Table 6 shows that none of the optimal HACHP will benefit from adding the additional high-pressure liquid circulation. However, for some of the cases the addition of the low-pressure liquid circulation does result in an increased performance for both the liquid line and suction line internal heat exchanger.

It should further be noted that most of these solutions result in an optimum low-pressure liquid circulation ratio of $f_2 = 0$, meaning that all the liquid extracted from the liquid-vapour separated should be circulated at the low-pressure. This is an interesting result as this means that the liquid pump should not be included in the cycle making the cycle layout simpler and cheaper to build. As seen, this configuration often results in COPs that are comparable to the SGHEX cycle. This cycle layout may thus also be a relevant solution. In the following this cycle configuration will be referred to as the evaporator liquid circulation heat pump ELCHP.

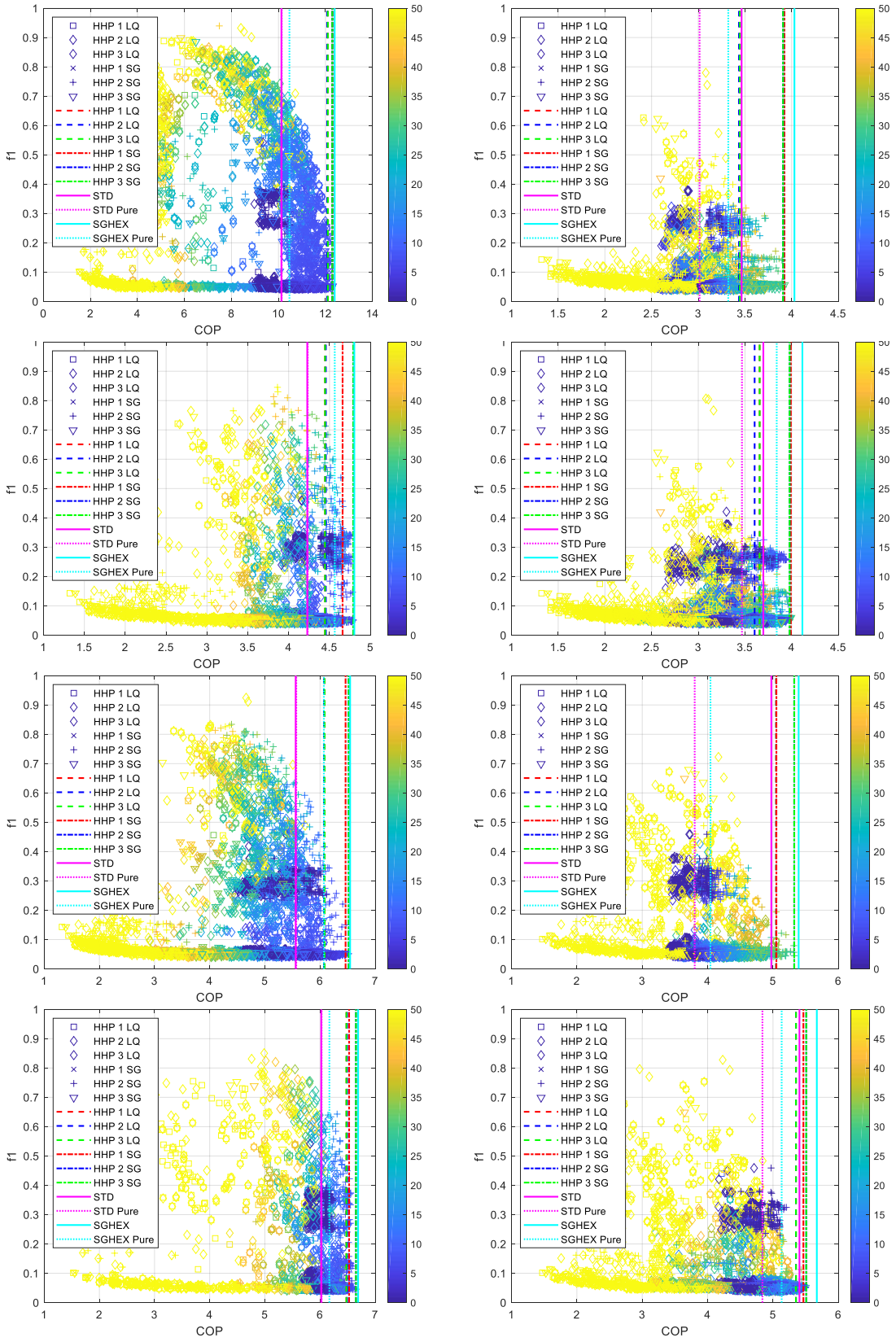

Figure 18. Relation between the COP and liquid circulation rate f_1 for cases I-VII and for all the suggested HACHP. Further, the best COP for the STD and SGHEX are indicated. The colourscale indicates the saturation temperature difference of the mixture.

Table 6. Results of the refrigerant screening, presenting the best working fluid for each cycle type and for all 8 operating conditions.

		Case 1							Case 2						
		COP	Fluid 1	Fluid 2	x_1	f_1	f_2	f_3	COP	Fluid 1	Fluid 2	x_1	f_1	f_2	f_3
	STD - Pure	10.14	R1233zd(E)	-	-	-	-	-	4.838	heptane	-	-	-	-	-
	STD	10.13	R1234ze(Z)	R1233zd(E)	0.9	-	-	-	5.405	pentane	heptane	0.7	-	-	-
	SGHEX - Pure	10.47	Heptane	-	-	-	-	-	5.133	heptane	-	-	-	-	-
	SGHEX	12.39	DEE	R1234ze(Z)	0.4	-	-	-	5.671	pentane	heptane		-	-	-
	HACHP	12.10	hexane	heptane	0.5	0.21	-	-	5.351	ipentane	heptane	0.6	0.05	-	-
LQ	HACHP LP circ.	12.10	hexane	heptane	0.5	0.21	1	-	5.351	ipentane	heptane	0.6	0.05	1	-
	HACHP HP circ.	12.10	hexane	heptane	0.5	0.21	-	1	5.351	ipentane	heptane	0.6	0.05	-	1
	HACHP	12.30	hexane	heptane	0.7	0.05	-	-	5.465	ipentane	hexane	0.5	0.05	-	-
SG	HACHP LP circ.	12.30	hexane	heptane	0.7	0.05	1	-	5.510	pentane	heptane	0.6	0.05	0.28	-
	HACHP HP circ.	12.30	hexane	heptane	0.7	0.05	-	1	5.465	ipentane	hexane	0.5	0.05	-	1

		Case 3							Case 4						
		COP	Fluid 1	Fluid 2	x_1	f_1	f_2	f_3	COP	Fluid 1	Fluid 2	x_1	f_1	f_2	f_3
	STD - Pure	6.028	R1234ze(Z)	-	-	-	-	-	3.802	heptane	-	-	-	-	-
	STD	6.022	R1234ze(Z)	R1233zd(E)	0.9	-	-	-	4.974	DME	DEE	0.4	-	-	-
	SGHEX - Pure	6.170	R1234ze(Z)	-	-	-	-	-	4.040	heptane	-	-	-	-	-
	SGHEX	6.691	pentane	R1234ze(Z)	0.3	-	-	-	5.392	pentane	heptane	0.5	-	-	-
	HACHP	6.479	hexane	heptane	0.4	0.05	-	-	5.049	ipentane	heptane	0.5	0.094	-	-
LQ	HACHP LP circ.	6.491	hexane	heptane	0.4	0.05	0	-	5.049	ipentane	heptane	0.5	0.094	1	-
	HACHP HP circ.	6.479	hexane	heptane	0.4	0.05	-	1	5.049	ipentane	heptane	0.5	0.095	-	1
	HACHP	6.527	hexane	heptane	0.4	0.05	-	-	5.052	hexane	R1234ze(Z)	0.6	0.05	-	-
SG	HACHP LP circ.	6.651	DEE	R1234ze(Z)	0.4	0.05	0	-	5.325	hexane	R1234ze(Z)	0.5	0.05	0	-
	HACHP HP circ.	6.527	hexane	heptane	0.4	0.05	-	1	5.052	hexane	R1234ze(Z)	0.6	0.05	-	1

		Case 5							Case 6						
		COP	Fluid 1	Fluid 2	x_1	f_1	f_2	f_3	COP	Fluid 1	Fluid 2	x_1	f_1	f_2	f_3
	STD - Pure	5.569	R1233zd(E)	-	-	-	-	-	3.467	heptane	-	-	-	-	-
	STD	5.558	R1234ze(Z)	R1233zd(E)	0.9	-	-	-	3.696	pentane	heptane	0.7	-	-	-
	SGHEX - Pure	6.070	heptane	-	-	-	-	-	3.840	heptane	-	-	-	-	-
	SGHEX	6.546	hexane	heptane	0.2	-	-	-	4.115	pentane	heptane	0.5	-	-	-
	HACHP	6.082	hexane	heptane	0.6	0.05	-	-	3.657	heptane	R1233zd(E)	0.2	0.05	-	-
LQ	HACHP LP circ.	6.082	hexane	heptane	0.6	0.05	1	-	3.657	heptane	R1233zd(E)	0.2	0.05	1	-
	HACHP HP circ.	6.082	hexane	heptane	0.6	0.05	-	1	3.657	heptane	R1233zd(E)	0.2	0.05	-	1
	HACHP	6.463	hexane	heptane	0.7	0.05	-	-	3.991	ipentane	heptane	0.6	0.05	-	-
SG	HACHP LP circ.	6.520	hexane	heptane	0.7	0.05	0	-	3.991	ipentane	heptane	0.6	0.05	1	-
	HACHP HP circ.	6.463	hexane	heptane	0.7	0.05	-	1	3.991	ipentane	heptane	0.6	0.05	-	1

		Case 7							Case 8						
		COP	Fluid 1	Fluid 2	x_1	f_1	f_2	f_3	COP	Fluid 1	Fluid 2	x_1	f_1	f_2	f_3
	STD - Pure	4.233	R1234ze(Z)	-	-	-	-	-	3.014	heptane	-	-	-	-	-
	STD	4.227	R1234ze(Z)	R1233zd(E)	0.9	-	-	-	3.463	DME	pentane	0.6	-	-	-
	SGHEX - Pure	4.563	heptane	-	-	-	-	-	3.321	heptane	-	-	-	-	-
	SGHEX	4.803	pentane	R1234ze(Z)	0.3	-	-	-	4.029	pentane	heptane	0.4	-	-	-
	HACHP	4.445	hexane	heptane	0.5	0.05	-	-	3.446	heptane	R1233zd(E)	0.2	0.05	-	-
LQ	HACHP LP circ.	4.455	hexane	heptane	0.5	0.05	0	-	3.446	heptane	R1233zd(E)	0.2	0.05	1	-
	HACHP HP circ.	4.445	hexane	heptane	0.5	0.05	-	1	3.446	heptane	R1233zd(E)	0.2	0.05	-	1
	HACHP	4.660	hexane	heptane	0.4	0.05	-	-	3.922	DEE	heptane	0.4	0.05	-	-
SG	HACHP LP circ.	4.791	hexane	heptane	0.4	0.05	0	-	3.922	DEE	heptane	0.4	0.05	1	-
	HACHP HP circ.	4.660	hexane	heptane	0.4	0.05	-	1	3.922	DEE	heptane	0.4	0.05	-	1

Finally, it may be seen from Table 6 that of the 21 fluids included in the screening only eight fluids are present in the optimum solutions. These fluids are the hydrocarbons: heptane, hexane, pentane and ipentane, the HFOs: R1233zd(E) and R1234ze(Z) and the finally: DME and DEE. It should be noted that many of the optimum solutions include heptane as one of the mixture components, especially for the HACHP. Often the mixture of heptane with either hexane or propane seems to yield high performance. This may indicate that close to optimum solution may be found for all operating conditions only by applying a small set of fluids. Ideally, just by altering the composition of a single mixture.

3.3.2.7. Discussion

As shown above, the results of the screening revealed that the best solution was always to apply the SGHEX cycle and further that for some cases a comparable performance could be attained by the advanced cycle layouts. It should be noted that none of the best options included the CO2/propane mixture which was the subject of the experimental investigation nor the standard HACHP with NH3/H2O which is currently the only commercially available solution for the advanced cycles.

Figure 19 compares the Lorenz efficiency of the best solution, determined by the combined refrigerant and cycle screening with the simulated results for a CO2/propane SGHEX cycle and a standard NH3/H2O HACHP cycle. Further, Figure 19 presents the Lorenz efficiency of the best standard cycle with a pure refrigerant. As seen neither the CO2/propane SGHEX cycle nor the standard NH3/H2O HACHP can reach the high performances identified by the combined refrigerant and cycle screening. The standard HACHP performed better than the STD pure cycle in all cases besides case 3, while the CO2/propane cycle was only better than the best pure cycle in cases: 3, 4, 7 and 8. It should be noted that the choice to test the CO2/propane mixture experimentally was decided based on operating conditions close to those of case 4 and as seen in this case the SGHEX cycle with the CO2/propane mixture gives a significant performance increase compared to the best pure fluid. However, even higher increases could be attained be applying the pentane/heptane mixture which was identified as the best mixture for this case. This again highlights the significant increases that can be attained by investigating the full set of possible solutions.

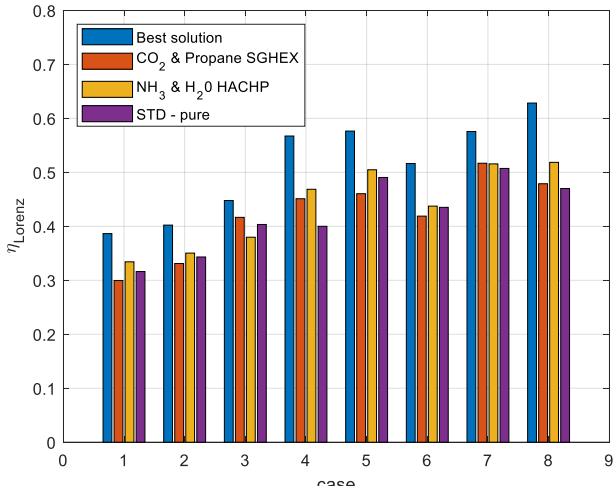

Figure 19. Lorenz efficiency of the best cycle and fluid combination, the SGHEX with a CO2 propane mixture as tested experimentally and NH3 H2O HACHP which is the only commercially available solution for the advanced cycle configurations. Further, the STD cycle with the best pure fluid is presented.

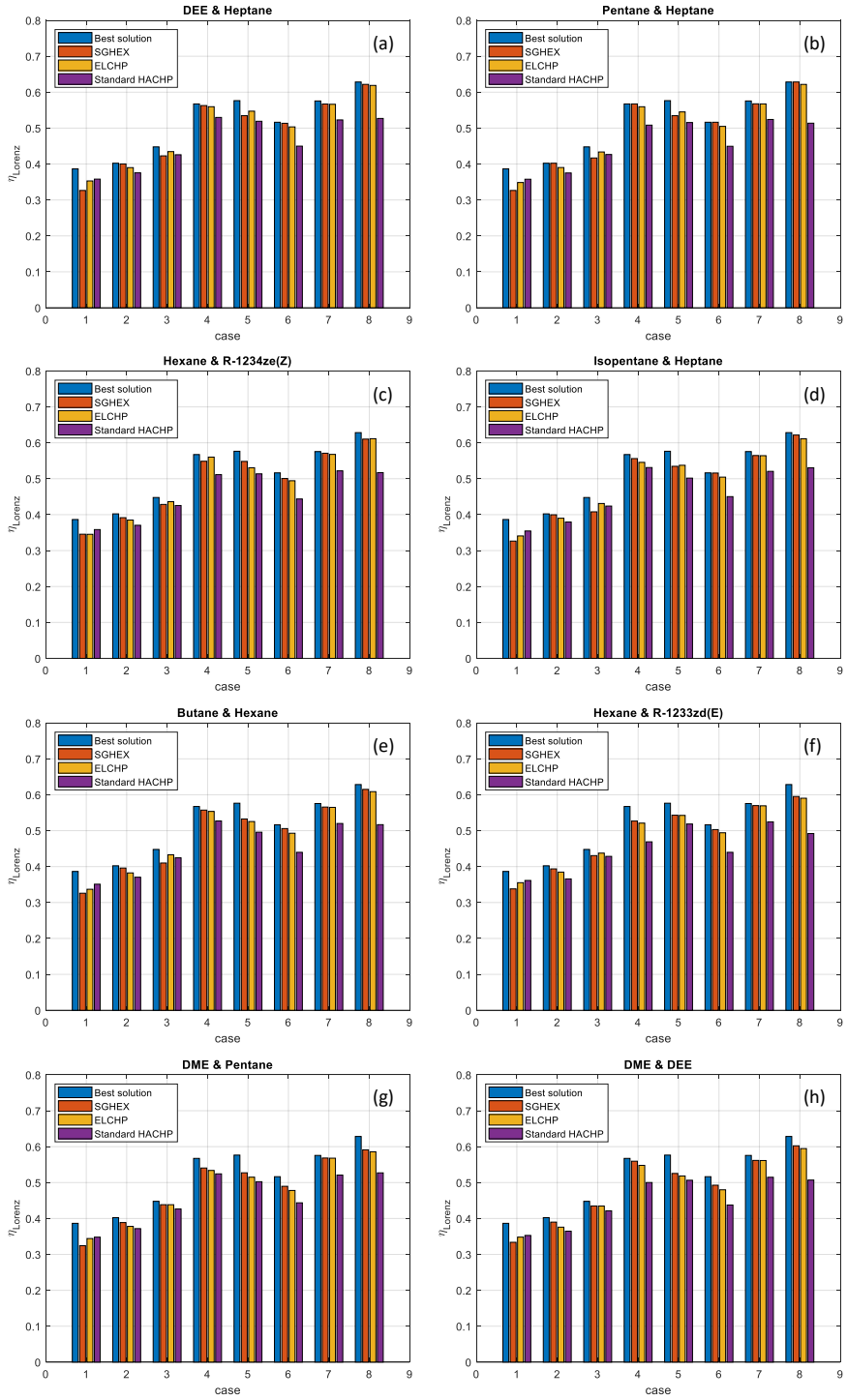

Figure 20. Lorenz efficiency of the eight best cycle and fluid combinations.

As also seen in the presented results, then although the best solutions encompass only eight of the 21 investigated fluids, this still requires a large variety of refrigerants including both hydrocarbons, HFOs and ethers. All of which may have their specific technical requirements and limitations. The large variety of refrigerants may thus be a limitation for the practical implementation of these high performance mixture heat pumps. It is thus relevant to discuss the possibility to identify near optimal solutions using only limited or even a single mixture. Ideally only changing the composition of a single mixture would yield a more practical and technically feasible solution.

Figure 20 compares the performance of a single mixture over all eight cases with the performance of the best identified solution. The results are presented for three different cycle layouts: the SGHEX cycle, the standard HACHP and the ELCHP, which was identified

during the screening. To clarify the ELCHP cycle corresponds the cycle seen in Figure 11(f) but without the liquid pump connecting the low pressure and high pressure sides, thus a cycle where all liquid extracted from the liquid vapour separator is circulated at the low pressure and supplied to the inlet of the evaporator. Further, Figure 20 presents this for eight different mixtures. These eight mixtures where selected as these give the highest average performance over all eight cases and the three included cycles. The mixture presented here were sorted from a-h in descending average performance.

As seen, none of the mixtures can attain exactly the optimal performance under for all cases but as seen it is possible to approach the optimum with a single mixture. It should further be noted that when investigating a single mixture, both the HACHP and ELCHP can results in higher performances than the SGHEX cycle. Generally, it is seen that the SGHEX for these selected mixtures is not a good match for case 1, here is seems that the HACHP is the more suitable solution. The ELCHP cycle generally results in a Lorenz efficiency that is comparable to the SGHEX cycle. Actually, for the two best mixtures DEE/Heptane and Pentane/Heptane the ELCHP has an average performance that slightly exceeds the SGHEX cycle.

4. Test of System

This section gives a general explanation of the considerations for design of the test set-up and of the purpose of the tests as well as the results.

The temperature sets used during the tests are not the same as used during the screening. The purpose of the screening was to elucidate the applicability of mixtures in a range of processes where there was either a large temperature change on both sides, or only on the warm side.

For testing a system solution was chosen which in the screening had shown to provide the largest efficiency. The choice of temperature set was based on considerations together with danARCTICA about the temperature set which is expected to have the largest market potential (20 ºC in and 10 ºC out on the cold side, and 40 ºC in and 70 ºC out on the warm side).

This also means that it is not possible directly to compare the COP from the screening with the COP from the tests, and also that the refrigerant mixture was not chosen as the one which in the screening proved to provide the largest COP.

The refrigerant mixture used for the tests was Propane / CO2, which is a well-known mixture used in other contexts and which the project group had experience with. In this section, calculations have also been made showing what the optimum COP could be based on measurements and calculations of the isentropic and volumetric efficiency of the compressor.

In general, one of the advantages of using a mixture is that it is possible to get the temperature curves on the two sides to match each other. It is "optimal" when the temperature curves on the two sides are parallel. If the temperature difference on the two sides is minimized, it is possible to reduce the LMTD (Log Mean Temperature Difference) as much as possible. However, one must keep in mind that in this connection, the area of the heat exchanger will of course be increased together with the investment costs.

The PI diagram of the plant is discussed and described in Appendix 1.

4.1. Design Considerations

All tests in the project have been focusing on the interaction between the evaporator and the suction gas heat exchanger. Normally, evaporators are configured to operate countercurrently, in order to include superheating also. If the temperature drop of the water in the evaporator is low, then it requires that the superheating on the refrigerant side is correspondingly low. Otherwise, there will be a drawback due to a lower evaporation temperature. To get an optimal function, it is also required that the refrigerant in the inlet port is distributed evenly so that each channel receives the same amount of liquid and gas. But this also means that if an evaporator operates with a relatively large superheating and the system operates with a constant water flow, then a part load condition will cause the evaporation temperature to be lowered.

In connection with a flooded evaporator, a liquid separator is always integrated in the refrigerant circuit between the evaporator and the compressor. The liquid separator is

intended to capture liquid droplets from the outlet of the evaporator. In principle, this mode of operation generates a superheating close to zero. Therefore, a higher evaporation temperature is achieved under part load – even with a constant water flow – since superheating does not limit the evaporation temperature upwards.

The temperature glide in the evaporator is here defined as the temperature difference between the temperature of the refrigerant at the inlet of the channel and of the saturated gas. Thus, in connection with binary mixtures, the pinch point can appear anywhere in the channel. This depends on the specific mixture combination. For pure refrigerants, the pinch point occurs either at the inlet or at the outlet, depending on whether there is superheating and depending on the size of this superheating.

For the tests are used a mixture of CO_2 and propane. Thereby, the temperature curve is convex, and depending on the mixture ratio and the superheating, the pinch point will appear at either the inlet or the outlet of the evaporator seen from the refrigerant side. Where the pinch point will appear also depends on whether or not a suction gas heat exchanger is used, and how many kW that comes through the suction gas exchanger. If there is an uneven distribution of refrigerant in the evaporator, the pinch point will not necessarily appear at the same place in all channels. The system has been operated with 5 %, 10 % and 15 % CO_2. The increasing concentration of CO_2 leads to an increasing temperature glide.

The evaporator is without an integrated distributor, but instead an external distributor is installed in the inlet manifold. The reason for choosing an external distributor is, primarily, that it has to be possible to easily replace the distributor with other models.

Since the distributor did not work optimally during the testing, the operation had to be done with a relatively large superheating – between 12 K and 14 K. The poor distribution has led to an uneven distribution above the plate pack, which has been confirmed with thermographic camera inspections.

The reason for this is probably impurities which are blocking the intended distribution along the distributor. An uneven distribution means that not all channels perform equally well. The consequence is that some channels are wet at the outlet, and others must be operated with so much superheating that the desired superheating for the whole unit can be provided.

The excess liquid from the outlet manifold also causes regulation problems, and therefore the placement of the sensor becomes a critical parameter. After all, the excess liquid can only evaporate through contact with the warm gas, and no matter what, it will take a while before this process is completed.

Therefore, it is important to take into account that the expansion valve sensor must be placed at a location where all the excess liquid has been evaporated. This will result in a time delay in the control of the system, which has to be compensated by the PID control. If not, there might be large challenges in getting the valve to be regulated properly. One solution to this problem is to increase the superheating, but this will cause a lower COP for the plant, which is obviously not appropriate.

The suction gas heat exchanger is installed with a bypass so that the evaporator can be operated with or without the integration of a suction gas heat exchanger, but also in a combination where only a part of the refrigerant flow through.

4.2. Operation of Tests

The tests were carried out by first running with full bypass on the suction gas heat exchanger and then by stepwise gradually leading more and more refrigerant through the suction gas heat exchanger. And as it will appear later, this will result in a higher and higher evaporation temperature and to an increasing COP.

The tests have been operated with a superheating between 12 K and 14 K. As previously discussed, this indicates that there have been challenges with the distribution in the evaporator. But an interesting finding from this poor distribution is that the suction gas heat exchanger has been playing an even more important role.

In the evaporator, the effect of the uneven distribution is quite dramatic, since the evaporation temperature compensates this by being lower than what was intended in the design. In a suction gas heat exchanger, on the other hand, an uneven distribution will play a more harmless role. The temperature of the condensate from the subcooler is typically so high that it easily will generate the desired superheating. It will be possible to generate an even higher superheating, which will result in a higher discharge temperature, and which can contribute to a reduction of the condensing temperature and provide an even higher COP.

In those channels which are dry at the evaporator outlet, there will be poor heat transfer rates. Therefore, by moving the two-phase area closer to the outlet, the heat flux will increase significantly in these channels, which totally will result in a more efficient evaporator.

In a suction gas heat exchanger, excess liquid from the evaporator will tend to run through the channels furthest away from the inlet. These channels are therefore the most loaded, and if the load is too large, the suction gas heat exchanger will not be able to convert all the liquid to gas. The unevaporated liquid will then pass through the sensor, which is obviously not desirable. This means that an appropriate choice of the suction gas heat exchanger is important - as well as how it is connected.

The temperature sensor for the expansion valve is installed on the suction gas pipe after the joining of the bypass and the outlet of the suction gas heat exchanger.

The heat pump has been operated as follows: The water side on the cold side of the heat pump has been connected to an electric resistance heating element, which, during test, was running with a constant output of 20 kW. The mass flow was continuously regulated to get a temperature difference of about 10 K. The outlet temperature of the water from the evaporator was regulated to be around 11 °C by adjusting the number of revolutions of the compressor.

The water on the hot side was adjusted to supply 70 °C out of the condenser and approx. 40 °C return to the subcooler. The water side was adjusted accordingly, to be approx. 70 °C at the outlet. The cooling to the 40 °C was provided by a dry cooler.

The compressor was controlled manually, and all tests started with the gas bypassed the suction gas heat exchanger. During all tests, the superheating ranged from 12 to 14 K, and unfortunately it has not been possible to reach below 12 K due to the reasons explained earlier.

4.3. Test Results

Figure 21 shows the temperatures and the quality of the refrigerant at the outlet with a CO_2 concentration of 5 %. The subsequent figures (Figure 23 and Figure 25) show results with CO_2 concentrations of 10 % and 15 %.

Temperatures are shown on the y-axis, and the time is shown on the x-axis. On the secondary y-axis to the right, the vapor quality is shown, and on the secondary x-axis at the top of the figures, the revolutions of the compressor are shown. The values representing the revolutions must be read in such way that the shown compressor speeds are only correct just before a change to a new value. It should be remarked that in the intervals, where the value does not change, there have been made adjustments of the speed. The shown values for the number of revolutions was read manually.

4.3.1. Results with 5 % CO_2

As previously mentioned, the relatively large superheating is caused by an unintentionally poor distribution in the plate pack. However, this helped to clarify the positive effect associated with integrating a suction gas heat exchanger into the refrigeration circuit.

In Figure 21, in the interval with 1288 revolutions per minute (RPM), it can be seen that the gas temperature out of the evaporator (Tr_ss_out) is close to 19 °C. The temperature is measured after the place where the bypass and the outlet from the suction gas heat exchanger meet. In a similar way, the temperature at the outlet from the evaporator (T_r_e_out) is calculated. This calculation corresponds well with the measured temperature (Tr_ss_out).

On Figure 21 T_r_dist shows the temperature after the throttling process across the distributor. This value is calculated and based on the measured pressure at the outlet of the evaporator. Therefore, the pressure drop across the channels is ignored, because it is relatively small compared to the pressure drop across the distributor. The value indicates the temperature of the refrigerant just before the inlet to the channels. Te_sat_vap indicates the saturated gas temperature. The low temperature means that all liquid has been evaporated. Thus, the temperature glide is found by subtracting Te_sat_vap by T_r_dist. That means, that the temperature glide is not a part of the superheating. It should also be noticed that the temperature difference increases over time, which is due to a decreasing quality at the inlet of the channels.

The quality X_r_e_out is a calculated value and indicates the gas condition at the outlet of the evaporator. The intervals where the superheating is larger than or equal to saturated gas are represented by a constant value of 0. When the conditions are in the two-phase region, the value in question is calculated correctly and will range from 1 to 0. However, a little liquid can appear at the outlet sight glass, even though the condition of the whole unit is actually superheated, due to an uneven distribution.

Each time a change occurs, it happens because of an active action which consists in changing the position of the bypass valve. In the first interval, which covers 1288 RPM, the bypass valve is fully open, and the shut-off valve is fully closed, in the branch pipe to the suction gas heat exchanger.

In the interval with 1179 RPM, the shut-off valve to the evaporator has been opened completely. This has caused a relatively rapid response in form of a higher suction pressure. The higher suction pressure, which results from a high saturation temperature given by Te_sat_vap, is the result of a reduced superheating zone. The reduced superheating in the evaporator will now be provided via the suction gas heat exchanger, which thereby cools the condensate corresponding to provide an energy balance of the suction gas heat exchanger. The fact that it has been able to reduce the revolutions from 1288 RPM to 1179 RPM with the same evaporator performance is caused by a higher suction pressure, and this has led to a larger specific volume of the gas for the compressor.

The interval 1152 RPM represents the process after a throttling process in the bypass pipe is completed, and which causes a greater amount of refrigerant to pass through the suction gas heat exchanger. Similarly, the suction pressure naturally increases, and it can read from the graph for the outlet quality, x_r_e_out, that the process is in the superheated area. However, through the sight glass installed at the outlet of the evaporator, it has been possible to observe that this is not the full truth. Here, it must be remembered that the value for the outlet quality has been calculated and that spot liquid droplets has been observed at the outlet, although the calculation shows that it should be superheated. The fact that there are liquid droplets is due to an uneven distribution of the refrigerant in the channels. This means that some channels are relatively superheated and that others run with a little overflow of liquid. The result is a superheating out of the evaporator of approx. 7 K. The figure shows that the total superheating is still in the interval from 12 to 14 K.

The figures also show the temperature of the refrigerant measured between the expansion valve and the distributor, called Tr_e_in. The temperature takes a dive every time the valve settings are changed. This happens because of an additional cooling of the condensate through the suction gas heat exchanger due to an increased load, since a larger amount of the refrigerant from the evaporator passes through the suction gas heat exchanger.

After another throttling process in the bypass, the refrigerant comes to the two-phase area at the outlet of the evaporator. Here the quality is approx. 0.98 which means that whether the process is running with a perfect distribution or not, it would still run with a little fluid at the outlet. The calculated value T_r_e_out_beregnet is corresponding to the level of Te_sat_vap.

After two further throttling processes, the compressor speed operates at 1070 RPM, and the result is that the outlet quality is approx. 0.94 and the Te_sat_vap is approx. 10 °C. The process started with a Te_sat_vap at approx. 5.5 °C, and thereby the saturation temperature is increased by not less than 4.5 °C by introducing a suction gas heat exchanger. It should be borne in mind, that the reason why the process was operated at such a low evaporating temperature is caused by a rather large superheating due to the fact that it was necessary to operate with a fairly poor distribution in the evaporator because of dirt in the distributor.

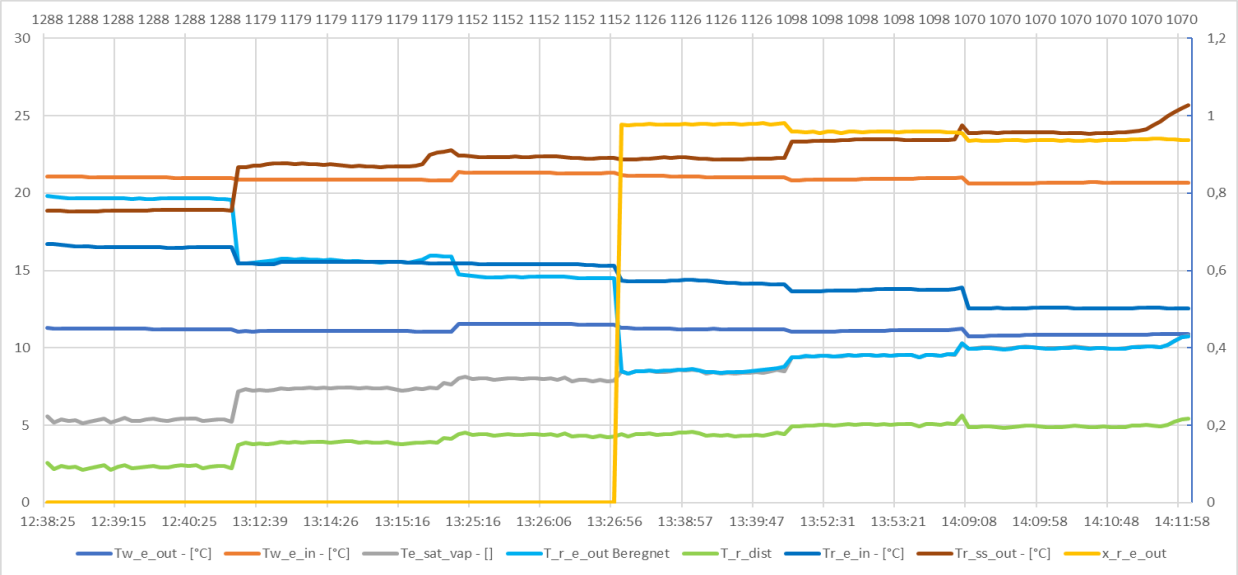

Figure 21. Temperatures (left side) and quality (x_r_e_out at right side) with 5 % CO_2.

However, despite the poor distribution, it does not cause that the channels run dry, which has been confirmed by inspections with a thermographic camera. The reason that the temperature is not higher than 5.5 °C, although the water out was approx. 11 °C, is solely due to the size of the heat exchanger. With a larger number of plates, the temperature could easily reach even higher, which will be illustrated later in this report through calculations.

It is important to remember that the outlet water temperature has not been kept constant at 11 °C. It has fluctuated about plus/minus half a degree. However, this does not change the fact that there has been achieved a considerable gain, and this must be seen in relation to the fact that it has been possible to raise the saturation temperature by not less than 4.5 K. And, as it can be seen the lowest water temperature occurs where the highest COP is obtained.

Figure 22 shows the COP of the heat pump and the heat transfer rate of the suction gas heat exchanger (Qsuc) during the same period as shown in Figure 21. Here, the COP is shown on the y-axis to the left, and the heat transfer rate is shown on the secondary axis to the right.

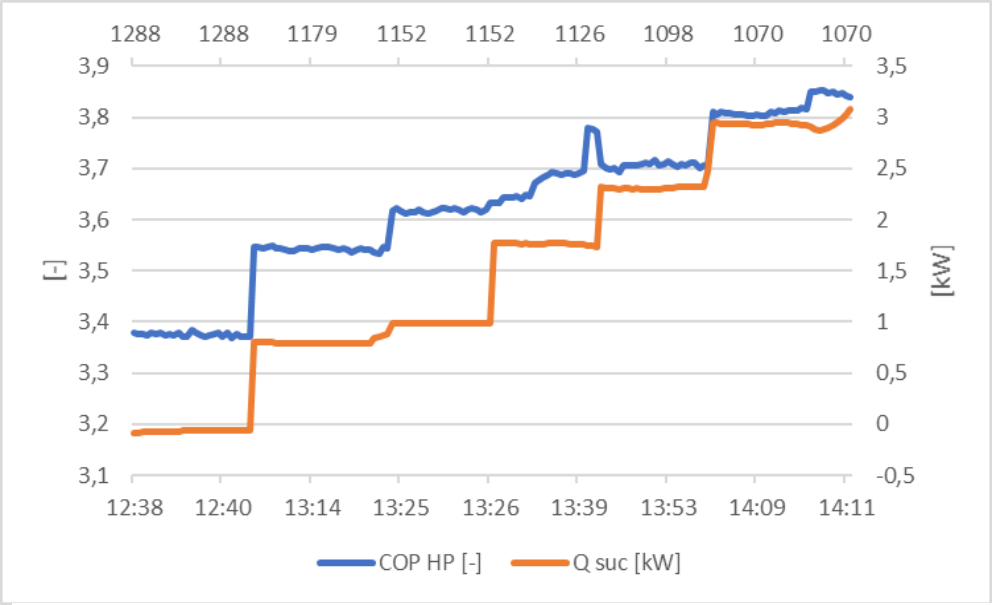

Figure 22. COP (at the left side) and Qsuc (kW, at the right side) with 5 % CO_2.

The result is a god correlation between COP and Qsuc. The COP at the start of the test was approx. 3.38, and at the end the value was close to 3.8. The result is that at the end Qsuc was 3 kW in the suction gas heat exchanger.

4.3.2. Results with 10 % CO_2

Figure 23 contains the same data as shown in Figure 21, but now with a concentration of 10 % CO_2. The procedure in this test is identical to the one with a concentration of 5 % CO_2. At the start there was a full bypass of the suction gas heat exchanger, and then gradually the refrigerant flow was increased. This test was divided in only 4 steps, whereas the previous one was divided in 6 steps. Otherwise, there is no difference in the test procedure.

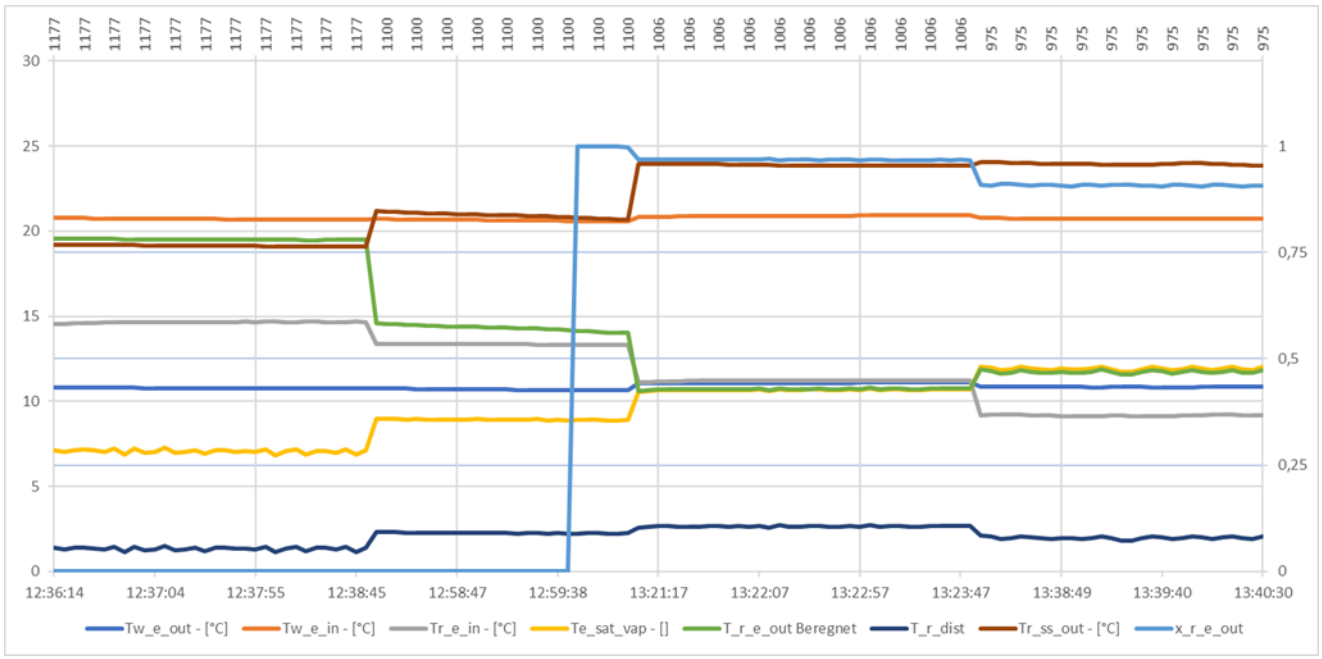

Figure 23. Temperatures (left side) and quality (x_r_e_out at right side) with 10 % CO_2.

In the interval of 1177 RPM, the first difference compared to Figure 21 can be observed. It is the glide of the refrigerant – this means the difference between the calculated temperatures of Te_sat_vap and T_r_dist – which is increased because of a larger amount of CO_2 in the mixture. Furthermore, it has been possible to reduce the revolutions from 1288 RPM to 1177 RPM, which is due to a change in the density and pressure of the refrigerant, since the evaporator capacity remain unchanged.

The superheating is adjusted so it is possible to run stable without the use of a suction gas heat exchanger. As it can be seen here, there might be a slightly lower superheating than during the 5% CO_2 test, see Figure 24. But it can also be seen that the temperature difference between Tw_e_in and Tr_ss_out is similarly slightly reduced.

It should be noted that at the end of the area marked with 1100 RPM, the tests end up by having saturated gas at the outlet of the evaporator, and the COP is increased from 3.3 to 3.5. When the compressor is running with a speed of 975 RPM the result is a COP of approx. 3.7 with a quality, x_r_e_ out, of 0.91. At the end the quality is lower than at the tests

with 5 % CO_2 It has not been possible to run with a quality of 100 % through neither 5 % CO_2 nor 10 % CO_2 without pendling of the system.

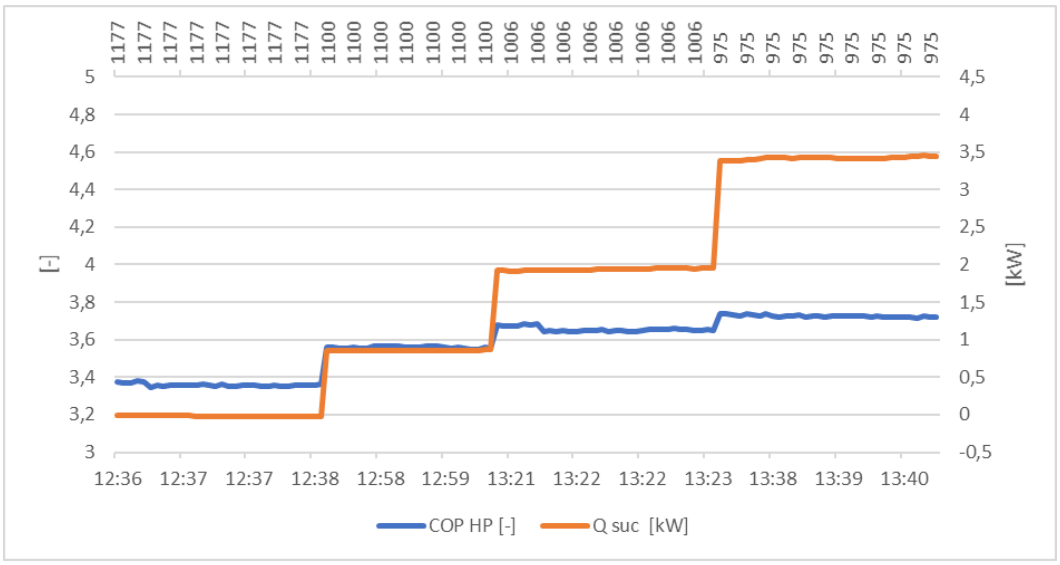

Figure 24. COP (at the left side) and Qsuc (kW, at the right side) with 10 % CO_2.

4.3.3. Results with 15 % CO_2

Figure 25 shows the results with 15 % CO_2. The figure shows that the tendency to reduce the difference between Tw_e_in and Tr_ss_out continues, and the difference between Te_sat_vap and T_r_dist is further increased.

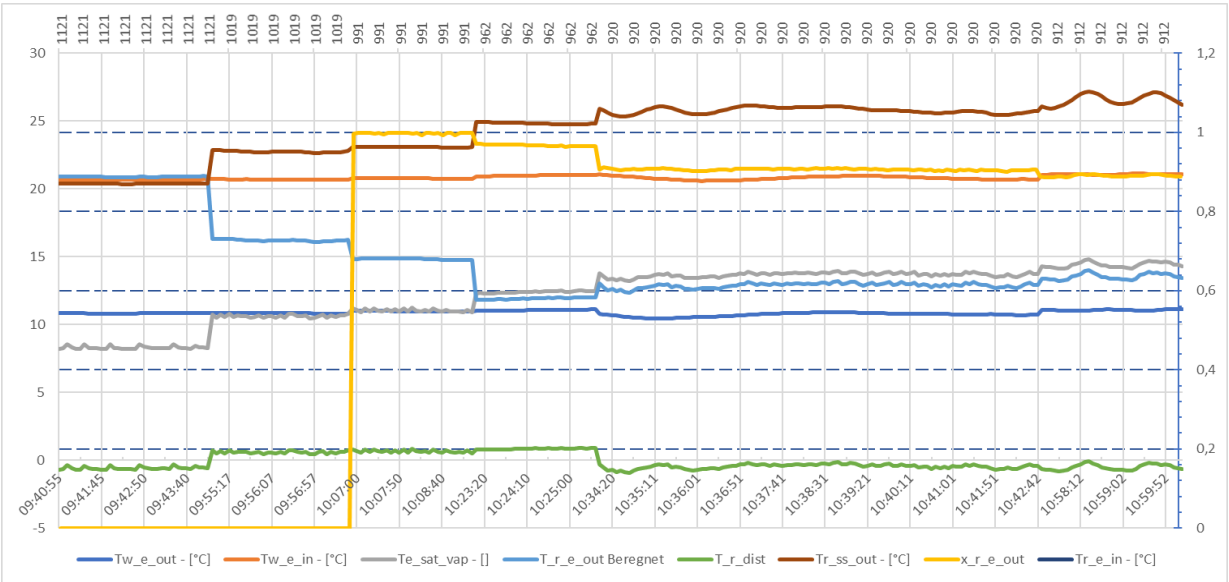

Figure 25. Temperatures (left side) and quality (x_r_e_out at right side) with 15 % CO_2.

The interesting point about the 15 % CO_2 test is that we have reached an outlet quality close to 90 % in the interval with 920 RPM. This corresponds to a heat transfer rate (Qsuc) in the suction gas exchanger of 3.5 kW, see Figure 26. Here, can a slight tendency for the system to fluctuate very weakly be seen. It has been tried to force a larger capacity into the suction gas exchanger than in the case of 920 RPM. But as shown in the interval with

912 RPM (See Figure 25), the system started fluctuating. It was not large fluctuations, and despite the fluctuations, the COP was slightly increased.

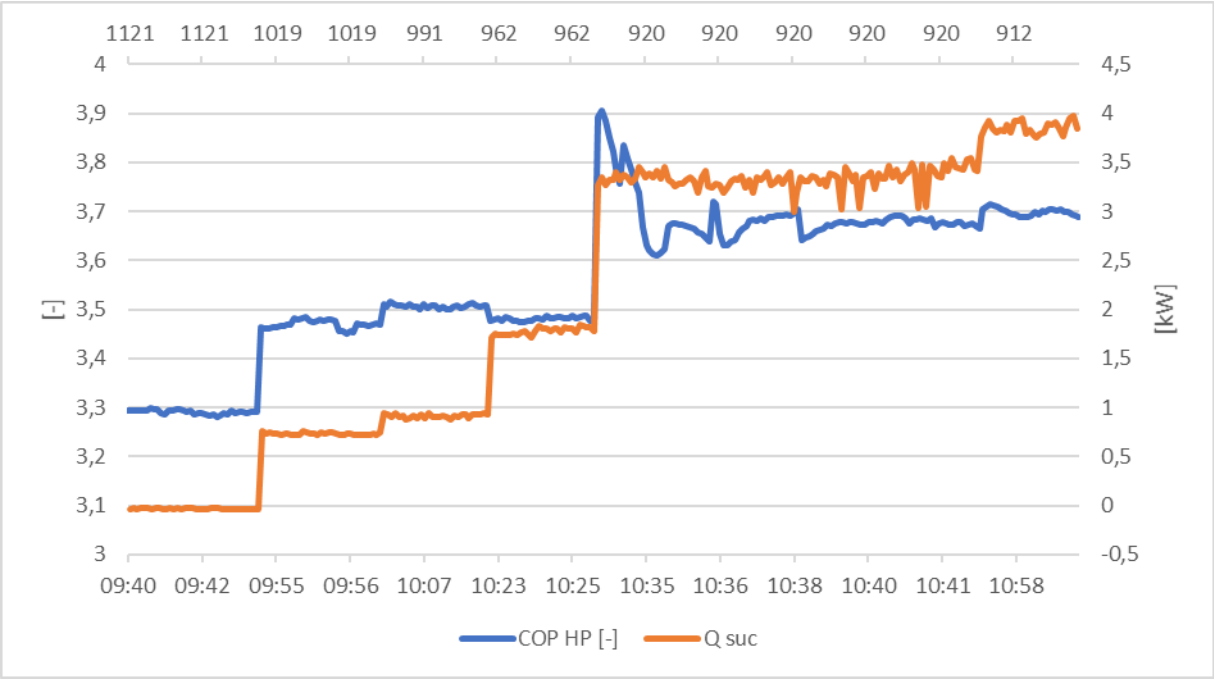

Figure 26. COP (at the left side) and Qsuc (kW, at the right side) with 15 % CO_2.

4.4. Evaluation of Test Results

The power consumption of the compressor has been measured as well as the mass flow of the water on the warm side, which led to the calculation of the mass flow of the refrigerant. And with a known compressor capacity and a measured speed, it was possible to calculate the isentropic efficiency and the volumetric efficiency. With this input plus the measured pressure and temperature, QT diagrams has been drawn by assistance of an EES model. For each concentration of CO_2, is the operating condition mapped in the first and last interval. In each interval, it is the operation condition just before switching to a new compressor speed that is shown in the figure. That is, in Figure 27, to the left, the operation condition with 5 % CO_2 and without the suction gas heat exchanger. In Figure 27, to the right, is the system operated with the highest capacity of the suction gas heat exchanger and with the same 5 % CO_2 concentration.

In the condenser as well as in the subcooler, the system is operated with very small temperature approaches. This also means that the water temperature out of the condenser is well above the saturated gas temperature. It is also clear that it has been possible to reduce the LMDT (Logarithmic Mean Difference Temperature) in the evaporator by integrating a suction gas heat exchanger in the refrigerant circuit. But even with the integration of a suction gas heat exchanger, there still are relatively poor temperature approaches, and this just reflects the significant potential by choosing a larger evaporator.

Furthermore, the diagrams in Figure 28 and Figure 29 clearly show how the glide of the refrigerant increases as a function of an increasing CO_2 concentration. Similarly, it is seen that there is a relatively small temperature approach between the gas from the evaporator

and the inlet water. This indicates that it is the large superheating that the regulator operates with that causes the relatively large LMDT. This is also reflected by the fact that it has been possible to increase the evaporator pressure to some extent by integrating a suction gas heat exchanger, which causes the superheating to be generated in the suction gas heat exchanger, and therefore it does not occupy space in the evaporator.

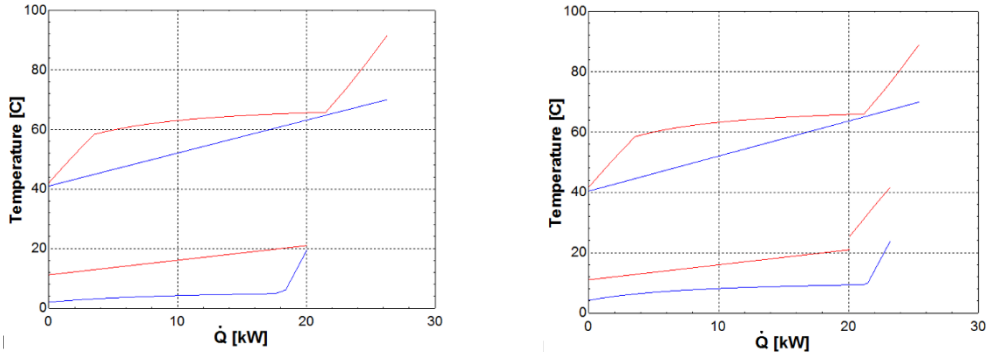

Figure 27. QT diagram for actual measurements with 5 % CO_2 without (left) and with (right) suction gas heat exchanger.

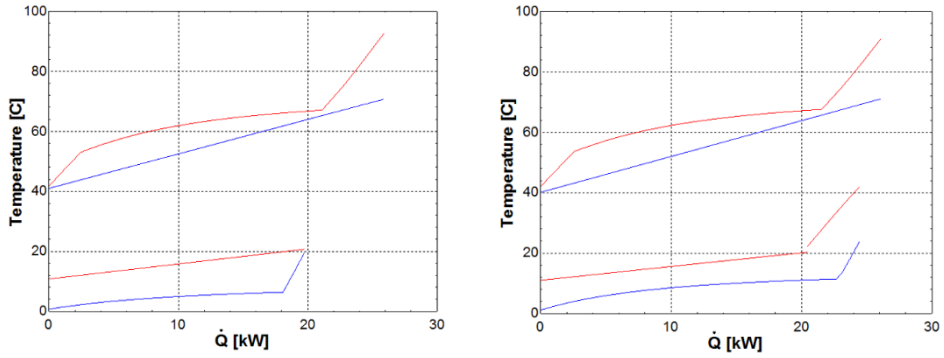

Figure 28. QT diagram for actual measurements with 10 % CO_2 without (left) and with (right) suction gas heat exchanger.

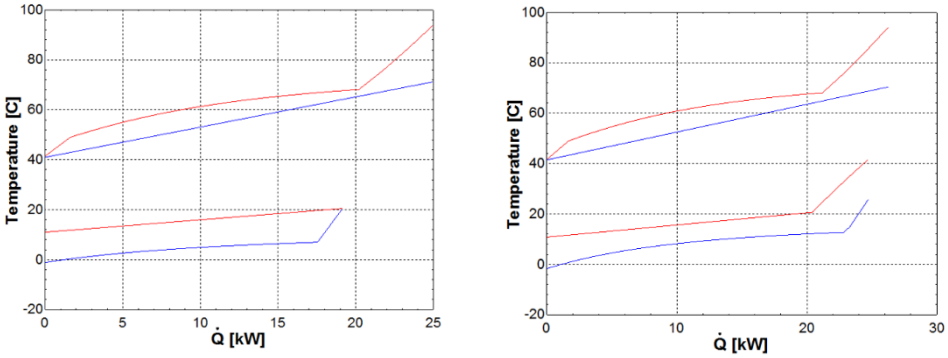

Figure 29. QT diagram for actual measurements with 15 % CO_2. without (left) and with (right) suction gas heat exchanger.

In the following figures (Figure 30– Figure 32), the evaporator pressure is being adjusted. The purpose is to see how high the COP will be in dependence of the actual water temperatures – with a temperature approach in the evaporator of about 1 K. This means, that the superheating – when operating without a suction gas heat exchanger – is adjusted, so the resulting temperature approach is approx. 1 to 2 K. The water temperatures have been the same as in the previous figures. The figures show that the superheating is going

towards zero, with an increasing CO_2 concentration, and at the same time, the pinch point is moving from the outlet of the water and towards the inlet.

The suction gas temperature of the compressor is raised to 35 °C when the system is operated with suction gas heat exchangers. The reason is that this provides a higher discharge temperature, and the result is also a lower condensing pressure and a higher COP. The heat loss coefficient from the compressor has been set to 20 %, which more or less corresponds to the measurements.

The performance of the suction gas heat exchanger has been maximized, so that the temperature out of the condensate from the suction gas exchanger corresponds approximately to the inlet temperature of the water.

Based on COP calculations for the three selected concentrations, it can be concluded that the values are quite close to the actual water temperatures. Therefore, it will be possible to boost the COP by an additional 10% compared to the measurements without a suction gas heat exchanger and by 9% compared to the calculations with a suction gas heat exchanger. And based on the measurements without a suction gas heat exchanger and the calculations with a suction gas heat exchanger, an improvement of 19% can be achieved in both cases.

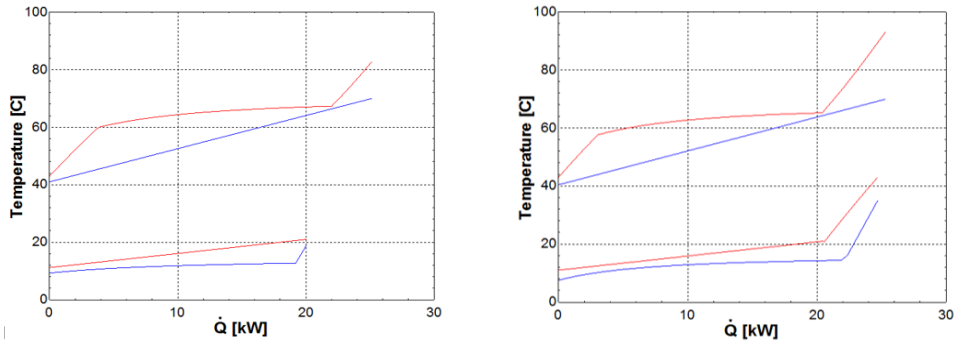

Figure 30. QT diagram with 5 % CO_2 and a minimal temperature approach (1 K in the condenser and 2 K in the evaporator) from actual measurements without (left) and with (right) suction gas heat exchanger.

Estimated COP in the case of 5 % CO_2:

COP without suction gas heat exchanger, Figure 30 to the left: COP = 3.92

COP with suction gas heat exchanger, Figure 30 to the right: COP = 4.22

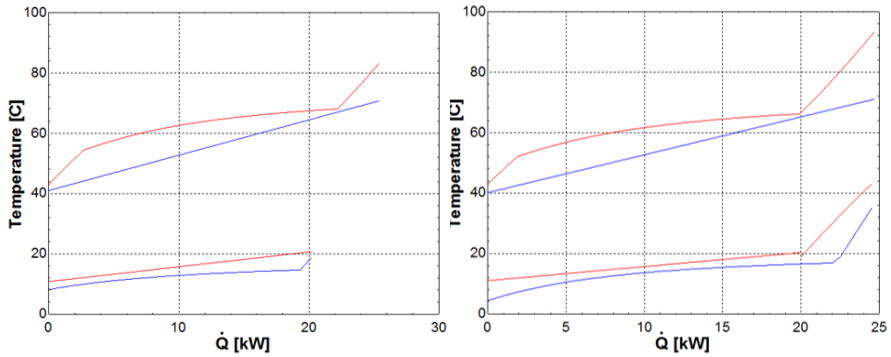

Figure 31. QT diagram with 10 % CO_2 and a minimal temperature approach (1 K in the condenser and 2 K in the evaporator) from actual measurements, without (left) and with (right) suction gas heat exchanger.

Estimated COP in the case of 10 % CO_2:

COP without suction gas heat exchanger, Figure 31 to the left: COP = 3.90

COP with suction gas heat exchanger, Figure 31 to the right: COP = 4.23

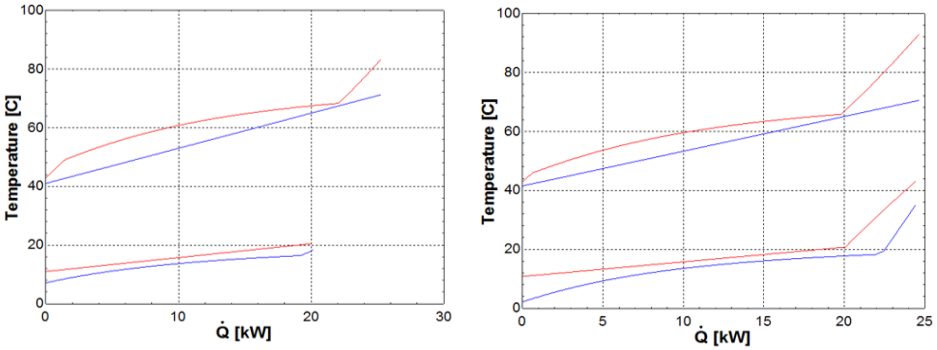

Figure 32. QT diagram with 10 % CO_2 and a minimal temperature approach (1 K in the condenser and 2 K in the evaporator) from actual measurements without (left) and with (right) suction gas heat exchanger.

Estimated COP in the case of 15 % CO_2:

COP without suction gas heat exchanger, Figure 32 to the left: COP = 3.88

COP with suction gas heat exchanger, Figure 32 to the right: COP = 4.22

5. Conclusion

The analyses performed in subtask 1, shown in chapter 3.2, demonstrated the performance increase possible by using zeotropic mixtures. The possible improvement in performance depends on the boundary conditions of the sink and the source and can be increased by avoiding superheating. A performance increase of up to 20 % with 5 K superheating or 27 % without superheating could be observed. Subtask 1 further shows that a good temperature match with sink and source can improve the performance significantly, while an optimal match does not necessarily result in an optimal COP.

Subtask 2, shown in chapter 3.3, identified several cycle layouts capable of increasing the glide match with the sink and the source and avoiding superheating in the evaporator. The identified cycles were the SGHEX cycle and the HACHP cycle. The HACHP cycle was further analysed with additional low and high pressure liquid circulation and two different internal heat exchanger placements.

All the identified cycle layouts where found to be capable of improving the performance of specific mixtures under specific operating conditions. However, it was also found that a number of mixtures suffered a reduction of COP when the advanced cycle layouts were imposed. The SGHEX cycle was found to be better than the STD cycle for all mixtures, compositions and operating conditions. This is mainly attributed to the avoidance of superheating in the evaporator and in part due to the reduction of throttling losses caused by the increased level of subcooling.

The screening performed in subtask 2 on all the advanced cycle layouts revealed that the best COP was always attained by the SGHEX. However, the fluid and the composition differed from case to case. Generally, the results of the refrigerant screening reveal that if the mixture can be chosen freely, then only the SGHEX cycle configuration should be considered. The SGHEX is also the simplest cycle that can avoid superheating. If, on the contrary, the mixture is selected a priori or from a limited set of options, then the advanced cycle layouts, namely the HACHP and the ELCHP, may be utilized to increase the performance.

The experimental part was executed at a test setup corresponding to the SGHEX-configuration. The purpose with the different tests was to document the benefit of using mixtures and to pinpoint the positive effect of the integration of the suction heat exchanger.

The tests were operated by the mixture propane/CO_2, and the mixture ratio was 5 %, 10 % and 15 % CO_2. All tests were performed by a capacity of 20 kW at the evaporator and a water temperature of 21 ^{0}C to 11 ^{0}C on the cold side and from 30 ^{0}C to 70 ^{0}C on the warm side. The superheating at the suction pipe connection of the compressor has been in the interval between 12 K to 14 K.

It has been possible to show that the COP is improved by 15 % to 20 % compared to a similar ammonia system. Furthermore, it has been shown that if the evaporator size was optimized to a temperature approach of 1 K, the COP could be increased by as much as 25 %. Finally, it has been shown that the introduction of suction gas heat exchangers not only improves the efficiency by having the superheating outside of the evaporator. It also has a positive impact on the efficiency of the evaporator by reducing the influence of an uneven distribution in the channels.

In order to compare the simulations and tests it can be seen that the simulations have shown a maximum improvement of up to 27 %, depending on the selected temperature set and mixture used. However, the tests are performed with a specific temperature set and mixture which have a smaller potential maximum performance than in the screening. Even though it was still possible to achieve an efficiency improvement of 15 % by the combination of Propane with CO_2 and by using a suction gas exchanger.

Appendix 1

Methodology – obtaining and the utilization of test results

A pilot setup of the zeotropic a heat pump was constructed to enable the collection of data and conduct research into the effectiveness of utilizing mixed refrigerants. A PI diagram of the zeotropic heat pump can be seen in Figure 33. The developed test heat pump consists of a single stage compression cycle with the addition of a sub-cooler and a suction heat exchanger. The heat sink and heat source are closed water loops, where the heat source is supplied by heating elements, whereas the heat sink utilized a secondary glycol circuit to absorb and then dispel the heat to ambient air. The heat pump has in addition to the gauges utilized by the PLC, separate gauges for the sole purpose of gathering performance data. This data has been utilized in order to ascertain the systems performance. The main purpose of this of the pilot heat pump is to measure the potential of zeotropic mixtures in practice and to further the development of mixed refrigerant heat pumps. Additionally, a key focus-point has been to determine the influence of the suction heat exchanger on the zeotropic heat pumps performance.

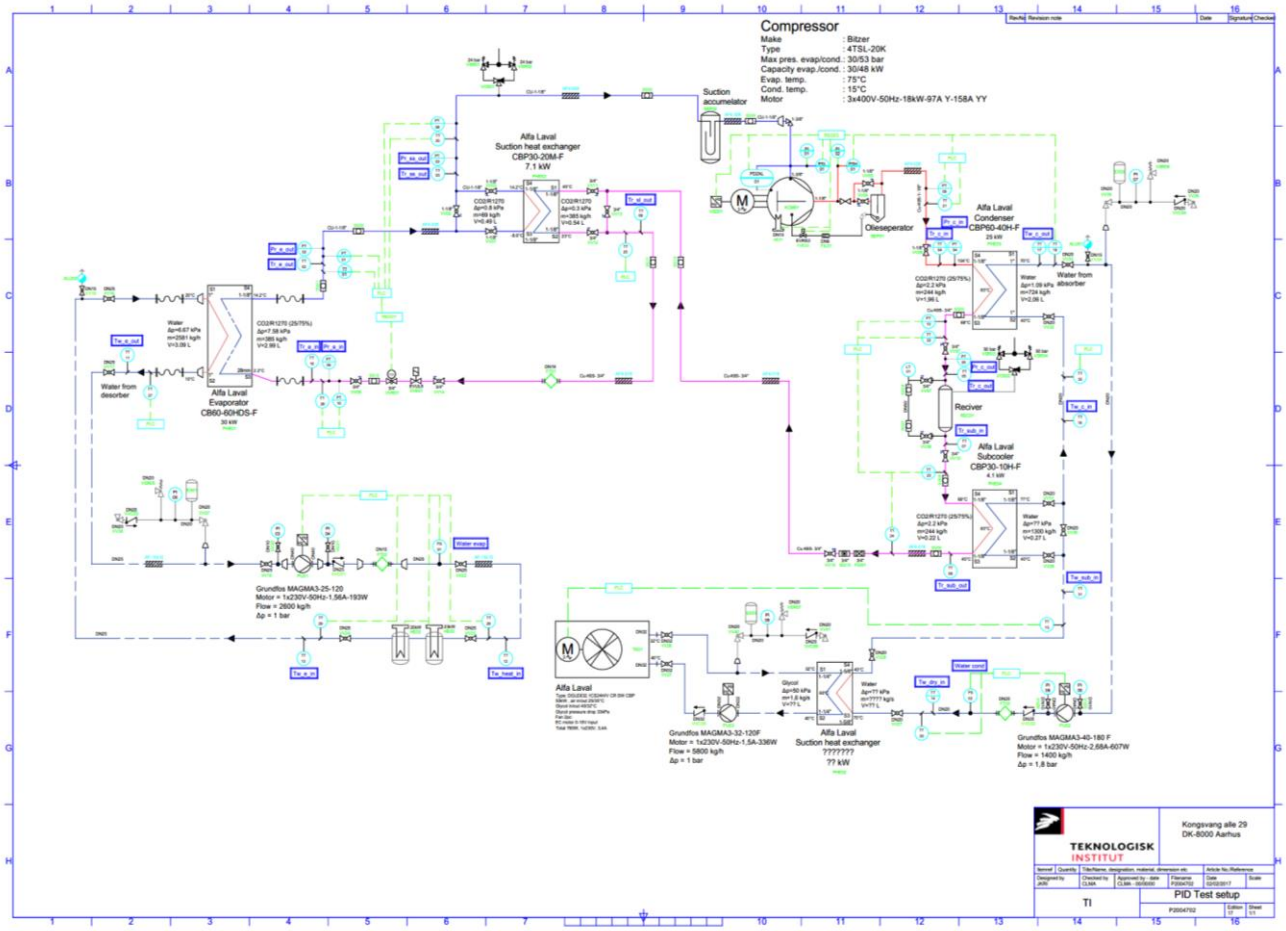

Figure 33. PI diagram of the zeotropic heat pump

The heat-pump has been fitted with temperature and pressure-gauges at key points in the circuit. Therefore, most of the state points have been obtained by utilizing the measured temperature and pressure gauges, the only exception being the point where two-phase

flow occurs. For instance, the state between the evaporator and the suction heat exchanger. When the suction heat exchanger is utilized the refrigerant becomes two-phase at this point. Therefore, a series of assumptions and an energy balance have been used to calculate this state-point.

Assumptions:

- The pressure-drop from exiting the condenser and until the expansion valve is assumed to be negligible.
- The heat exchangers are assumed to be adiabatic
- Conservation of mass

In order to calculate the state-point between the evaporator and the suction heat exchanger, all of the above assumptions have been utilized. Therefore, the energy balance can be reduced to the changes in enthalpy on both sides being equal and determining the state point after the evaporator.

$$h_{comp_{in}} - h_{evap_{out}} = h_{suc_{in}} - h_{suc_{out}}$$

Where:

$h_{comp_{in}}$ = Enthalpy into compressor [kJ/kg]

$h_{evap_{out}}$ = Enthalpy out of the evaporator[kJ/kg]

$h_{suc_{in}}$ = Enthalpy into the suction heat exchanger [kJ/kg]

$h_{suc_{out}}$ = Enthalpy out of the suction heat exchanger [kJ/kg]

The refrigerant mass flow ($\dot{m}_{ref}$) is determined by assuming that the energy absorbed by the heat sink is equal to the energy rejected from the refrigerant in the condenser. By establishing an energy balance for the suction heat exchanger, it will be possible to determine the refrigerant mass flow:

$$\dot{m}_{ref} = \frac{\dot{Q}_{suc}}{\left(h_{suc_{in}} - h_{suc_{out}}\right)}$$

Where:

$\dot{Q}_{suc}$ = energy rate transferred in the suction heat exchanger [kW]

In order to calculate the performance of the compressor, i.e. the volumetric efficiency and the isentropic efficiency, the displacement rate is needed to calculate the volumetric efficiency and is the product of the volume, number of cylinders and rotational speed (rpm).

$$\dot{V}_{displacement\ rate} = \frac{\pi}{4} \cdot d^2 \cdot s \cdot z \cdot \frac{N}{60}$$

Where:

d = cylinder diameter [m]

s = stroke [m]

z = number of cylinders [-]

N = compressor rotational speed, rpm

The volumetric efficiency is calculated as the relation between the actual displaced volume and the potential displacement.

$$\eta_V = \frac{\dot{m}_{ref} \cdot v(T_{suc} \cdot P_{suc})}{\dot{V}_{displacementrate}}$$

Where:

$\dot{m}_{ref}$ = refrigerant mass flow [kg/s]

v = specific volume of the refrigerant [m³/kg]

T_{suc}= Suction Temperature [°C]

P_{suc} = Suction pressure [bar]

The isentropic efficiency is calculated by the isentropic compression in relation to the measured work of the compressor.

$$\eta_{is} = \frac{\dot{m}_{ref} \cdot (h_{2_s} - h_1)}{\dot{W}_{Komp}}$$

Where:

$\dot{m}_{ref}$ = refrigerant mass flow [kg/s]

h_{2_s} = Enthalpy derived from isentropic compression [kJ/kg]

h_1=Enthalpy at the suction line of the compressor [kJ/kg]

$\dot{W}_{Komp}$ = Electrical power consumption of the compressor [kW]

The coefficient of performance (COP) has been calculated by dividing the heat received in the heat sink with the electrical consumption of the compressor.

$$COP = \frac{\dot{Q}_{heat}}{\dot{W}_{Komp}}$$

Where:

COP = Coefficient of performance [-]

$\dot{Q}_{heat}$ = Heat flow rate [kJ/s]

The acquisition of the measured data and the equations in this lay the basis for the subsequent analysis.

Appendix 2. References

During the project two papers have been written and published. The title of the first paper is:

Analysis of temperature glide matching of heat pumps with zeotropic working fluid mixtures for different temperature glides

Benjamin Zühlsdorf a), Jonas Kjær Jensen a), Stefano Cignitti b), Claus Madsen c), Brian Elmegaard a).

a): Department of Mechanical Engineering, Technical University of Denmark, Nils Koppels Alle, Building 403, 2800 Kgs. Lyngby, Denmark

b): Process and Systems Engineering Center (PROSYS), Department of Chemical and Biochemical Engineering, Technical University of Denmark, Søltofts Plads, Building 229, 2800 Kgs. Lyngby, Denmark

c): Danish Technological Institute, Gregersensvej, 2630 Taastrup, Denmark

The abstract of the paper is:

The present study demonstrates the optimization of a heat pump for an application with a large temperature glide on the sink side and a smaller temperature glide on the source side. The study includes a numerical simulation of a heat pump cycle for binary mixtures based on a list of 14 natural refrigerants. This approach enables a match of the temperature glide of sink and source with the temperature of the working fluid during phase change and thus, a reduction of the exergy destruction due to heat transfer. The model was evaluated for four different boundary conditions. The exergy destruction due to heat transfer, which is solely caused by the fluid having a non-ideal temperature profile was quantified and an indicator describing the glide match was defined to analyze its influence on the performance. The results indicated, that a good glide match can contribute to an increased performance. The increase in performance was dependent on the boundary conditions and reached up to 20 % for a simple cycle and up to 27 % if the superheating can be avoided. The temperature glide match in the source was identified to have a higher influence on the performance than in the sink.

Published in: Energy 153 (2018) 650 - 660.

The title of the second paper is:

Heat pump working fluid selection—economic and thermodynamic comparison of criteria and boundary conditions with authors: Benjamin Zühlsdorf, Jonas Kjær Jensen, Brian Elmegaard from Department of Mechanical Engineering, Technical University of Denmark, Nils Koppels Allé, Bygning 403, 2800 Kgs. Lyngby, Denmark.

The abstract of the paper is:

The study analyzes approaches for the selection of working fluids for the design of heat pump cycles based on numerical modeling. Different approaches for defining economically reasonable assumptions for the heat exchanger dimensioning were compared with respect to the identification of thermodynamically and economically promising working fluids. It was revealed that comparisons based on fixed heat exchanger investment do not exploit the performance of potentially high performing fluids. The approach of defining the pinch point temperature differences in the heat exchangers was found to provide results that were closest to the economic optimum, while being readily applicable in screening procedures. The method was demonstrated by two examples using excess heat from data centers for district heating supply. For the two cases, zeotropic mixtures were identified that could improve the thermodynamic performance by 30 %–35 % while achieving a reduction of levelized cost of heat of 8 % to 10 %.

Published in: International Journal of Refrigeration. 98 (2019) 500–513.